

**GROUNDWATER FLOWPATHS IN THE MANGROVE SYSTEM SURROUNDING
BOVONI LANDFILL WITHIN THE ST. THOMAS EAST END RESERVES (STEER):
A PILOT STUDY**



Kristin Wilson, Ph.D., Wells National Estuarine Research Reserve, Wells, ME
Andrew Reeve, Ph.D., University of Maine, Orono, ME
Renata Platenberg, Ph.D., University of the Virgin Islands, St. Thomas, VI

March 31, 2014

Water Resources Research Institute
University of the Virgin Islands

Disclaimer

The research on which this report is based was financed in part by the U.S. Department of the Interior, United States Geological Survey, through the Virgin Islands Water Resources Research Institute. The contents of this publication do not necessarily reflect the views and policies of the U.S. Department of the Interior, nor does mention of trade names or commercial products constitute their endorsement by the United States Government.

Acknowledgements

The authors wish to thank the Virgin Islands Waste Management Authority for allowing site access and supporting field logistics; the Virgin Islands Department of Planning and Natural Resources and the United States Geological Survey Water Resources Research Institute at the University of the Virgin Islands for funding this project; Jessica Keller (University of the Virgin Islands, Marine & Environmental Science graduate student) and Anne Marie Hoffman (The Nature Conservancy, St. Thomas, VI) for their work in the field; Dr. Paul Jobsis (Center for Marine and Environmental Science, University of the Virgin Islands, St. Thomas, VI), Ms. Alina Mathew (College of Science and Mathematics, University of the Virgin Islands, St. Thomas, VI), and Dr. Henry Smith (Water Resources Research Institute, University of the Virgin Islands) for their assistance with project logistics; University of Maine's Sawyer Environmental Chemistry Laboratory for their timely analyses of water chemistry samples; and Mr. Paul Dest (Wells National Estuarine Research Reserve) for his support of Dr. Wilson's time working on this project.

TABLE OF CONTENTS

	<i>Page No:</i>
List of Figures	4
List of Tables	8
List of Acronyms	9
Abstract	10
1. INTRODUCTION	11
1.1. Background	11
1.2. Study Site: St. Thomas East End Reserve (STEER) and Bovoni Landfill	11
1.3 Landfills and Coastal Ecosystems	15
2. PROBLEM DESCRIPTION	16
3. METHODOLOGY	18
3.1. Study Site	18
3.2. Sediment Coring	19
3.3. Groundwater Monitoring	19
3.3.1. Monitoring Well Installation	19
3.3.2. Hydraulic Head Measurement	20
3.3.3. Water Chemistry	20
3.3.4. Temperature Monitoring and Analysis	21
4. FINDINGS	22
4.1. Sediment Cores	22
4.2. Groundwater Hydrology	22
4.3. Water Chemistry	41
5. CONCLUSIONS AND RECOMMENDATIONS	44
Bibliography	45

LIST OF FIGURES

Page No:

- Figure 1: Map showing the eastern portion of St. Thomas (see map inset), the St. Thomas East End Reserve boundary (shaded light blue), and contributing watersheds (outlined in orange).12
- Figure 2: Red mangroves (*Rhizophora mangle*) within Mangrove Lagoon, St. Thomas, VI.13
- Figure 3: Map of the study area (approximate area outlined in blue). Points labelled a-c indicate the locations of pictures included in Figure 4.14
- Figure 4: (a) Piles of trash and tires on the entrance road to Bovoni Landfill, looking west, (b) Bovoni Landfill with dump truck ascending as viewed from an open-water area within a dead area of black mangroves (*Avicennia germinans*) adjacent to Bovoni Landfill, looking west and (c) The study area as viewed from near the top of Bovoni Landfill, looking to the northeast. Approximate point locations of these photographs are shown in Figure 3.....15
- Figure 5: Open areas within the mangrove fringe adjacent to Bovoni Landfill seem to have appeared over the last 11 years as these Google Earth images from March 3, 2002 (top) and February 2, 2013 (bottom) show. Images taken in the field in January 2014 (right) document standing dead mangrove stems in multiple areas that appear forested in the 2002 image.17
- Figure 6: Location of study area and position of well clusters in the mangrove fringe adjacent to Bovoni Landfill. Well locations and site numbers are indicated with red dots and adjacent numbers. Each site includes both a shallow (5 ft.) and deep (10 ft.) well, except for site 7 which just includes a shallow well. Aerial photograph from Google Earth November 29, 2006.18
- Figure 7: (a) Surface water ditch sampled along the road directly adjacent to the landfill. (b) A trench across the road drained the surface water ditch in (a) into the upland of the mangrove fringe pictured in (c). (c) Upland vegetation leading into the study region (mangrove fringe below). All pictures taken January 9, 2014 by K. Wilson.21
- Figure 8: Hydraulic head measurements collected from shallow (1 m deep) wells on

February 13, 2014. Equipotentials (dashed red curves) and flow directions (blue arrows) interpreted from the hydraulic head data are superimposed on the well data.23

Figure 9: Hydraulic head measurements collected from deep (2.5 m deep) wells on February 13, 2014. Equipotentials (dashed red curves) and flow directions (blue arrows) interpreted from the hydraulic head data are superimposed on the well data.24

Figure 10: Hydraulic head measurements collected from shallow (1 m deep) wells on March 6, 2014. Equipotentials (dashed red curves) and flow directions (blue arrows) interpreted from the hydraulic head data are superimposed on the well data.25

Figure 11: Hydraulic head measurements collected from deep (2.5 m deep) wells on March 6, 2014. Equipotentials (dashed red curves) and flow directions (blue arrows) interpreted from the hydraulic head data are superimposed on the well data.26

Figure 12: Groundwater temperature data collected at site 5 from February 13 to February 26, 2014. Data were collected at the interface between surface water and sediment (black line), and at depths of 7 cm (blue dots), 14 cm (green dots) and 21 cm (red dots). Blue, green, and red lines display results from a one-dimensional heat transport model at depths of 7, 14, and 21 cm calibrated to the data by varying the groundwater velocity and sediment porosity. The computer simulation best matched the field data when porosity was set to 34% and groundwater velocity was -9.6×10^{-6} m/sec (discharge or upward flow).27

Figure 13: Groundwater temperature data collected at site 7 from February 13 to February 26, 2014. Data were collected at the interface between surface water and sediment (black line), and at depths of 7 cm (blue dots), 14 cm (green dots) and 21 cm (red dots). Blue, green, and red lines display results from a one-dimensional heat transport model at depths of 7, 14, and 21 cm calibrated to the data by varying the groundwater velocity and sediment porosity. The computer simulation best matched the field data when porosity was set to 53% and groundwater velocity was -7.1×10^{-6} m/sec (discharge or upward flow).28

Figure 14: Groundwater temperature data collected at site 1 from February 13 to February 26, 2014. Data were collected at the interface between surface water and sediment (black line), and at depths of 7 cm (blue dots), 14 cm (green dots) and 21 cm (red

dots). Blue, green, and red lines display results from a one-dimensional heat transport model at depths of 7, 14, and 21 cm calibrated to the data by varying the groundwater velocity and sediment porosity. The computer simulation best matched the field data when porosity was set to 20% and groundwater velocity was -1.7×10^{-5} m/sec (discharge or upward flow).29

Figure 15: Groundwater temperature data collected at site 2 from Feb. 13 to Feb 26, 2014. Data were collected at the interface between surface water and sediment (black line), and at depths of 7 cm (blue dots), 14 cm (green dots) and 21 cm (red dots). Blue, green, and red lines display results from a one-dimensional heat transport model at depths of 7, 14, and 21 cm calibrated to the data by varying the groundwater velocity and sediment porosity. The computer simulation best matched the field data when porosity was set to 46% and groundwater velocity was -8.0×10^{-6} m/sec (discharge or upward flow).30

Figure 16: Time series of hydraulic head data at site 1 from January 9 to March 06, 2014 measured manually (dots) and recorded with a data logging pressure transducer (lines). Hydraulic head in shallow (red) wells are typically lower than in deep (blue) wells, indicating groundwater discharge at this location to the mangrove swamp.31

Figure 17: Time series of hydraulic head data at site 2 from January 9 to March 6, 2014 measured manually (dots) and recorded with a data logging pressure transducer (lines). Hydraulic head in shallow (red) and deep (blue) wells indicating vertical groundwater flow at this location oscillates from recharge to discharge over time. Low hydraulic head values in the deep well (before Feb 02., 2014) are due to the slow influx of water into the well after installation as the well equilibrated.32

Figure 18: Time series of hydraulic head data at site 4 from January 7 to March 6, 2014 measured manually (dots) and recorded with a data logging pressure transducer (lines). Hydraulic head in shallow (red) well is lower than that in the deep (blue) well indicating groundwater discharge at this location to the mangrove swamp. Low hydraulic head values in the shallow well (before Jan 29., 2014) are due to the slow influx of water into the well after installation as the well equilibrated.33

Figure 19: Time series of hydraulic head data at site 5 from January 9 to March 6, 2014

measured manually (dots) and recorded with a data logging pressure transducer (lines). Low hydraulic head values in the shallow (red) well (entire plot) are due to the slow influx of water into the well after installation as the well equilibrated.34

Figure 20: Time series of hydraulic head data at site 6 from January 9 to March 6, 2014 measured manually (dots) and recorded with a data logging pressure transducer (lines). Manual hydraulic head measurements indicate hydraulic heads in the deep (blue) well are lower than in the shallow well, indicating groundwater discharge at this location to the mangrove swamp. The data logging pressure transducer installed in the deep well appears to be malfunctioning and is not recording reasonable hydraulic head data.35

Figure 21: Time series of hydraulic head data at site 7 from January 9 to March 6, 2014 measured manually (dots) and recorded with a data logging pressure transducer (line).36

Figure 22: Time series of hydraulic head data at site 10 from January 7 to March 6, 2014 measured manually (dots) and recorded with a data logging pressure transducer (lines). Hydraulic head in shallow (red) well is lower than that in the deep (blue) well indicating groundwater discharge at this location to the mangrove swamp.37

Figure 23: Time series of hydraulic head data at site 11 from January 7 to March 6, 2014 measured manually (dots) and recorded with a data logging pressure transducer (lines). Hydraulic head in shallow (red) well is varies above and below than that in the deep (blue) well indicating shifts in the direction of vertical groundwater flux at this location. Low hydraulic head values in the deep well (before January 29, 2014) are due to the slow influx of water into the well after installation as the well equilibrated.38

Figure 24: Time series of hydraulic head data at site 13 from January 7 to March 6, 2014 measured manually (dots) and recorded with a data logging pressure transducer (lines). Hydraulic head in shallow (red) well is usually lower than that in the deep (blue) well indicating groundwater discharge to the mangrove swamp. Oscillations in shallow well data occur twice a day and appear to be related to ocean tides.39

Figure 25: Time series of hydraulic head data at site 13 from January 7 to March 6, 2014

measured manually (dots) and recorded with a data logging pressure transducer (lines). Hydraulic head in shallow (red) well is usually lower than that in the deep (blue) well indicating groundwater discharge to the mangrove swamp. Oscillations in shallow well data occur twice a day and appear to be related to ocean tides.40

Figure 26: Total dissolved nitrogen concentrations measured at monitoring well locations and a surface ditch near the Bovoni Landfill. The ‘Ditch’ sample and the shallow sample at site 5 were collected from surface water and all other samples were collected from groundwater wells.42

LIST OF TABLES

Table 1: Surface water salinities collected in the field on January 9, 2014 varied across the study area. The handheld meter did not record salinity at sites 4, 6, and 13.41

Table 2: Specific conductance and pH for water samples. All data were measured on the day of collection using handheld electrical probes (1/9/2014). Calibration of the pH meter was done using pH 4 and 7 standards. Calibration of the specific conductance meter was done using standards with conductivities of 1., 1.9, and 18 mS/cm.41

Table 3: Chemistry data for filtered (0.45 um) water samples. Chemical analyses were performed at the University of Maine’s Sawyer Environmental Chemistry Laboratory. Metals analyses were completed by Inductively Coupled Plasma Atomic Emission Spectroscopy and Total Dissolved Nitrogen (TDN) analysis was performed with an ALPKEM flow solution IV autoanalyzer. RL stands for Recording Limit.44

LIST OF ACRONYMS

DPNR	Department of Planning & Natural Resources
EPA	Environmental Protection Agency
GPS	Global Positioning System
LOI	Loss on Ignition
NOAA	National Oceanic and Atmospheric Administration
PVC	Polyvinyl chloride
RL	Recording Limit
STEER	St. Thomas East End Reserves
TDN	Total Dissolved Nitrogen
TNC	The Nature Conservancy
USGS	United States Geological Survey
UVI	University of the Virgin Islands
VIWMA	Virgin Islands Waste Management Authority

ABSTRACT

The St. Thomas East End Reserve (STEER) includes 9.6 km² of “significant coastal, marine and fisheries resources” on the southeastern end of St. Thomas. Mangrove Lagoon, within STEER, contains the island’s largest intact stand of mangroves and is considered one of St. Thomas’ most important fish nurseries and an eco-tourism locations. Bovoni Landfill, an unlined landfill in operation since 1979 and under consent decree for non-compliance since 2012, abuts Mangrove Lagoon on the western edge of STEER. Water that infiltrates and percolates through landfill waste, produces leachate, a liquid that can contaminate groundwater, compromising human and ecological health. This pilot study measures groundwater chemistry, flowpaths, and flux rates across the mangrove system adjacent to Bovoni Landfill within Mangrove Lagoon and STEER. Preliminary results from hydraulic head data indicate that shallow groundwater flows toward the center of the mangrove swamp, where open water occurs. Hydraulic head measured in deeper wells indicates flow toward the southern portion of the wetland and outward toward the ocean. The majority of the sites have upward hydraulic gradients, indicating groundwater is discharging to the mangrove swamp. Rapid increases in water levels were recorded in data logging pressure sensors on January 28, February 22, February 26, 2014 indicating rapid influx of water into the mangrove swamp occurs during the highest tides and during high rainfall events. Water chemistry data (total dissolved nitrogen and heavy metals (zinc, chromium, lead, nickel, and tin)) reveal that surface water pathways may be more important in the delivery of contaminants to the mangrove fringe than groundwater pathways. Future work should: (1) continue monitoring efforts to understand the relationship between groundwater flowpaths and standing dead mangrove and open-water features, (2) increase the spatial and temporal resolution of water chemistry sampling, (3) process archived geologic cores to better understand potential stratigraphic controls of groundwater flowpaths, and (4) use computer models like USGS SEAWAT and FiPy to test alternative assumptions regarding groundwater flow. These findings are of direct management concern to STEER, Virgin Islands Waste Management Authority, Department of Planning and Natural Resources, and the Environmental Protection Agency.

GROUNDWATER FLOWPATHS IN THE MANGROVE SYSTEM SURROUNDING BOVONI LANDFILL WITHIN THE ST. THOMAS EAST END RESERVES (STEER): A PILOT STUDY

1. INTRODUCTION

1.1. Background

Coastal wetlands are located at the intersection of the terrestrial upland and the marine environment and are particularly sensitive to environmental change (Valiela et al., 2001; Orth et al., 2006). Mangrove ecosystems are one type of coastal wetland and are intertidal, forested areas found along low-energy shorelines (Valiela et al., 2001). These estuarine habitats are ecologically valuable, supporting a diversity of wildlife, ecosystem, and economic functions (e.g., shoreline stabilization and infrastructure protection, export of organic material to nearshore environments, nursery habitat for coral reef organisms, eco-tourism opportunities; Valiela et al., 2001). Despite their value, mangroves worldwide and especially in the USVI, are threatened by development and changing land use (Valiela et al., 2001; Conservation Data Center, 2010). In addition, they receive far less attention in the scientific literature and general media compared to other coastal habitats, like coral reefs (Costanza et al. 1997; Orth et al. 2006). This suggests that more work should focus on these systems, including interactions and linkages with adjacent terrestrial environments, including freshwater contributions delivered via groundwater.

1.2. Study Site: St. Thomas East End Reserves (STEER) and Bovoni Landfill

The St. Thomas East End Reserves (STEER) includes 9.6 km² of “significant coastal, marine and fisheries resources” on the southeastern end of St. Thomas (STEER, 2011; Figure 1). STEER includes Mangrove Lagoon, Cas Cay, St. James, and the Compass Point Marine Reserves and Wildlife Sanctuaries and contains mangrove forests, salt ponds, lagoons, reefs, and cays. STEER’s vision is to “restore and maintain a functional coastal ecosystem that promotes sustainable recreational opportunities and compatible commercial uses with community engagement through effective management” (STEER, 2011). STEER ecosystems provide essential habitat for many bird and marine species, some of which are commercially valuable (STEER, 2011).



Figure 1. Map showing the eastern portion of St. Thomas (see map inset), the St. Thomas East End Reserve boundary (shaded light blue), and contributing watersheds (outlined in orange). From, horsleywitten.com/STEERwatersheds/pdf/Maps/Watersheds.pdf

Mangrove Lagoon within STEER, contains the island’s largest intact stand of mangroves and is considered one of St. Thomas’ most important fish nurseries (STEER, 2011; Figures 1-3). It also supports eco-tourism opportunities through kayak and snorkel expeditions (Virgin Island Ecotours, 2012). Two of St. Thomas’ largest watersheds empty into Mangrove Lagoon both of which are highly developed with residential and commercial infrastructure, including the Bovoni Landfill along STEER’s western border (Figures 1, 3).



Photo: K. Wilson 2014

Figure 2. Red mangroves (*Rhizophora mangle*) within Mangrove Lagoon, St. Thomas, VI.



Figure 3. Map of the study area (approximate area outlined in blue). Points labelled a-c indicate the locations of pictures included in Figure 4.

The Bovoni Landfill is an unlined landfill that covers approximately 330 acres of which 40 acres border mangrove ecosystems along the western edge of STEER (Figures 3, 4). The landfill has been in operation since 1979, accepting solid waste from St. Thomas and St. John, since the 1990s (Virgin Islands Waste Management Authority (VIWMA), 2012). It is managed by VIWMA whose mission is to “protect public health and the natural beauty of the environment for residents and visitors” (VIWMA, 2012) and whose vision is to “provide territory-wide collection, treatment and disposal services in a manner that will preserve the environment for future generations” (VIWMA, 2012). Currently, Bovoni Landfill is under Consent Decree for violating previously-issued federal orders regulating its operation. Bovoni Landfill is set to close in 2014 (Federal Register, 2012); it is unknown at this time if the Landfill will meet that closure date and how environmental impacts resulting from its operation may extend beyond that time.



Figure 4. (a) Piles of trash and tires on the entrance road to Bovoni Landfill, looking west, (b) Bovoni Landfill with dump truck ascending as viewed from an open-water area within a dead area of black mangroves (*Avicennia germinans*) adjacent to Bovoni Landfill, looking west, and (c) The study area as viewed from near the top of Bovoni Landfill, looking to the northeast. Approximate point locations of these photographs are shown in Figure 3.

1.3 Landfills and Coastal Ecosystems

In the United States, landfills are the most common method of solid-waste disposal (EPA, 2010) and in densely-populated, small-island nations they can be especially problematic (e.g., Jones, 2010). Water that infiltrates and percolates through landfill waste produces leachate, a liquid that can contaminate groundwater, compromising human and ecological health (Klinck and Stuart, 1999). Leachate can be toxic and often contains dissolved organic matter (methane and volatile fatty acids), inorganic macro components, heavy metals (e.g., cadmium, arsenic, lead), and anthropogenic organic compounds (e.g., aromatic hydrocarbons; Christensen et al., 1994).

Leachate originating from landfills may impact groundwater and surface water that discharges to coastal wetlands (Quinn et al. 2005; Gobler and Boneillo, 2003). The resulting terrestrial impact

on coastal water quality has the potential to alter these neighboring biological communities and may be a long-term stressor to coastal ecosystems because groundwater is one link that consistently connects terrestrial and nearshore areas (Dosis et al., 2011; Gobler and Boneillo, 2003). Despite this, very few studies examine the effects of landfills on marine ecosystems (e.g., Pope et al. 2011; Quinn et al. 2005; Gobler and Boneillo, 2003). This study adds to this growing body of work, while also providing data in support of management decisions for Mangrove Lagoon made by STEER, VIWMA, the Virgin Islands Department of Planning and Natural Resources (DPNR), and the Environmental Protection Agency (EPA).

2. PROBLEM DESCRIPTION

In general, there have been very few studies on the effects of landfills on marine ecosystems (but see, Pope et al. 2011; Quinn et al. 2005; Gobler and Boneillo, 2003). In addition, preliminary results of the chemical contaminant and bioeffects assessment in sediments at 24 locations within STEER by the National Oceanic and Atmospheric Administration (NOAA) reveal consistently higher levels of contaminants (polycyclic aromatic hydrocarbons, polychlorinated biphenyls, total extractable hydrocarbons, tributyltin, chromium, cadmium, lead, mercury, nickel and zinc) within Mangrove Lagoon compared to other sampled areas within STEER. However, because of the stratified random design of the sampling scheme, the source(s) of these contaminants remain unclear (Tony Pait, NOAA, personal communication, STEER Core Planning Committee, 9/3/2012). Furthermore, apparent loss of mangroves adjacent to Bovoni Landfill from 2002-2013 (Figure 5) are of management concern (Anne Marie Hoffman, The Nature Conservancy (TNC), personal communication).



Figure 5. Open areas within the mangrove fringe adjacent to Bovoni Landfill seem to have appeared over the last 11 years as these Google Earth images from March 3, 2002 (top) and February 2, 2013 (bottom) show. Images taken in the field in January 2014 (right) document standing dead mangrove stems in multiple areas that appear forested in the 2002 image.

This pilot study measures groundwater chemistry and flowpaths across the mangrove system adjacent to Bovoni Landfill within Mangrove Lagoon and STEER (Figure 3). Not only are these questions of interest scientifically, but they also are of direct management concern to STEER, VIWMA, DPNR, and the EPA. This work provides important data to support management decisions on St. Thomas, while also informing the management of landfills in other coastal locations. The study also establishes a baseline for potential long-term monitoring past the closure date of the landfill. By providing data to reinforce management decisions, this study supports important drivers of St. Thomas' economy, including eco-tourism opportunities and fisheries health. Finally, the work trains one graduate student from UVI (Jessica Keller) in aspects of geology, an area of study for which there are no upper-level courses currently offered.

3. METHODOLOGY

3.1 Study Site

The study area targets the mangrove fringe adjacent to Bovoni Landfill (Figure 3) within the area of apparent mangrove decline since 2002 (Figure 5). This area includes living red mangroves (*Rhizophora mangle*; located closest to Mangrove Lagoon and in the spur in the center of the study area), living black mangroves (*Avicennia germinans*), standing dead black mangrove with stems denuded of vegetation, open-water features, and open muddy areas. Groundwater well locations were selected to maximize understanding of potential groundwater flowpaths across the study region.

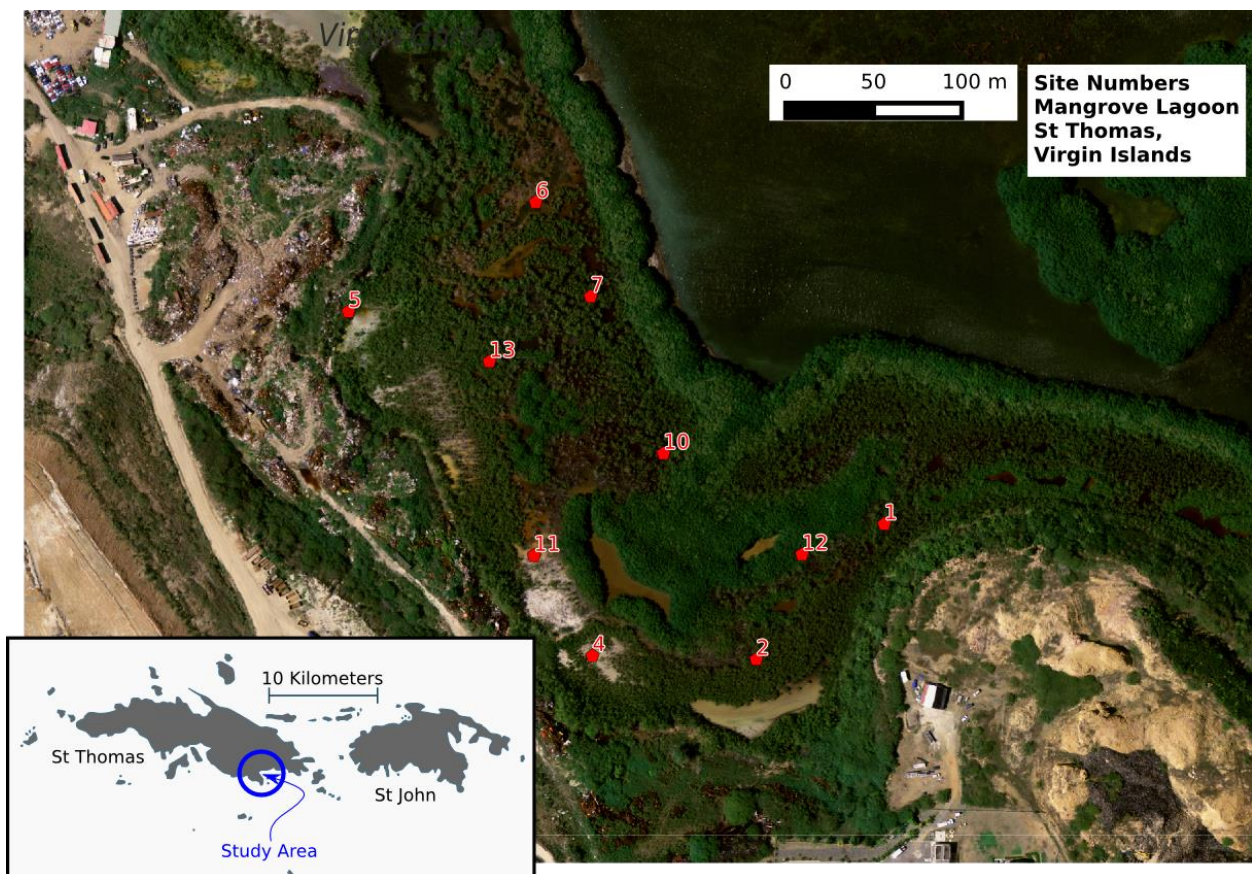


Figure 6. Location of study area and position of well clusters in the mangrove fringe adjacent to Bovoni Landfill. Well locations and site numbers are indicated with red dots and adjacent numbers. Each site includes both a shallow (5 ft.) and deep (10 ft.) well, except for site 7 which just includes a shallow well. Orthophotographs from U.S. Geological Survey (<http://cumulus.cr.usgs.gov>) published Dec. 2010.

3.2 Sediment Coring

To place the groundwater measurements within a geophysical context we collected nine, 1-2 m Eijkelkamp “Dutch” hand-auger cores at all sites except site 12. Cores were not collected at site 12 because the sediment was so wet that material was lost from the bottom of the core barrel and was unable to be retrieved. Cores were brought back to the lab and archived for future analyses by UVI graduate student, Jessica Keller for her Masters thesis (beyond the time frame of this pilot study).

3.3 Groundwater Monitoring

3.3.1 Monitoring Well Installation

From January 5-11, 2014, Dr. Kristin Wilson, Dr. Andrew Reeve, Ms. Anne-Marie Hoffman (TNC), and Ms. Jessica Keller (graduate student, UVI), worked to install 19 groundwater wells in 10 locations (Figure 5) spread across the mangrove fringe adjacent to Bovoni Landfill. Wells were constructed from 2.54 cm nominal diameter flush threaded PVC pipe with 30 cm machine slotted screens. For all sites except 7, both a shallow (5 foot total length) and deep (10 foot total length) well were installed.

Upon installation, all wells were developed by inserting a one half inch (1.27 cm) diameter PVC pipe fitted with a nylon brush to scrub the well and surge water within the well. Water and sediment within the well were then cleared using hand-held pumps and allowed to re-charge. Nineteen non-vented data logging pressure transducers (Solinst leveloggers) were deployed (one per well), along with one barometric pressure sensor to correct for changes in atmospheric pressure (site 11). Wells were installed January 7-8, 2014 and all data loggers downloaded (and re-started) on January 9 to make sure they were functioning correctly. Data loggers have since been downloaded and are working properly (late January, Keller) with the exception of the data logger in the deep well at site 6.

Four wells were surveyed using a Trimble NetR9 global positioning system (GPS) with Zephyr II geodetic antenna to establish the absolute position of the wells and provide reference points for manual surveying. The GPS data were post-processed using the GPS Precise Point Positioning internet service operated by Natural Resources Canada, Geodetic Survey Division. All wells (top of pipe) were manually surveyed using a Berger 32x Automatic Level and stadia rod to determine the relative elevation differences between wells and GPS coordinates for all wells were recorded with a hand-held GPS unit.

3.3.2 Hydraulic Head Measurement

The depths to water in monitoring wells were manually measured on February 13 and March 6, 2014 using an electrical water-level indicator to characterize spatial patterns in vertical and horizontal hydraulic gradients. These data were converted to hydraulic head by subtracting the measured water depths from the surveyed elevation of each well.

Water pressures were autonomously measured at 20-minute intervals using non-vented data logging pressure and temperature sensors installed in all wells. These data were converted to water levels (height above sensor) by subtracting atmospheric pressure, recorded using a separate barometric pressure sensor, from the total water pressure and then correlating the sensor measurements to manual hydraulic head measurements.

3.3.3 Water Chemistry

Water samples were collected from shallow and deep wells at sites 1, 2, 4, 5, and 11 using a hand vacuum pump fitted to an erlenmeyer flask. These well clusters were chosen for initial water chemistry analyses because of their relative proximity to the landfill compared to other well sites. Samples were collected from wells, decanted into 60 ml plastic containers, and placed in a cooler on ice. Two surface water samples, one at site 5 and the other in a ditch adjacent to the landfill (Figure 7), were collected by directly dipping the 60 ml plastic container into standing water. Surface water at site 5 was collected because of a recorded “chemical smell” when flushing the well during installation (K. Wilson, field notes, January 2014).



Figure 7. (a) Surface water ditch sampled along the road directly adjacent to the landfill. (b) A trench across the road drained the surface water ditch in (a) into the upland of the mangrove fringe pictured in (c). (c) Upland vegetation leading into the study region (mangrove fringe below). All pictures taken January 9, 2014 by K. Wilson.

Specific conductance and pH were measured using electrical probes in all water samples on the same day they were collected (January 9, 2014). Specific conductance (or salinity) of surface water at different sites were measured in the field as well. All water samples were transported to the Sawyer Environmental Chemistry Laboratory at the University of Maine, filtered (0.45 micrometer), and analyzed for total dissolved nitrogen, lead, zinc, tin, nickel, copper and chromium. Heavy metals analysis was performed using Inductively Coupled Plasma Atomic Emission Spectroscopy and nitrogen was analyzed using an ALPKEM flow solution IV autoanalyzer.

3.3.4 Temperature Monitoring and Analysis

At four sites (1, 2, 5 and 7), we installed a vertical array of four thermochron ‘i-button’ temperature sensors to record daily temperature fluctuations to infer shallow groundwater flow (Anderson, 2005). I-buttons were deployed in February 2014 for a 13-day period. Vertical

groundwater flow rates were estimated from this temperature data by fitting a one-dimensional heat transport model to the data. This one-dimensional heat transport model was based on the explicit finite-difference method with upwind difference method used for the convection term (Jaluria, 1996). This computer model simulates the conduction, convection, and dispersive transport of heat. Fixed temperature boundary conditions were assigned to the top (based on measured temperatures) and bottom of the model domain. The computer model was created using the Python scripting language (van Rossum and Drake, 2001), and calibrated to field data using the L-BFGS-B algorithm (Zhu et al., 1997) available in the Scipy computational library (Jones et al., 2001).

4. FINDINGS

4.1 Sediment Cores

Preliminary observations in the field reveal more inorganic clay-rich sediment in cores collected closer to the landfill with increasing organic-rich peats dominating cores collected further from the landfill. UVI graduate student, Jessica Keller, will describe these cores as part of her Masters' thesis (beyond the time frame of this pilot study).

4.2 Groundwater Hydrology

Hydraulic head data (Figures 8-11) indicate shallow groundwater flows toward the center of the mangrove swamp, where open water occurs. Hydraulic head measured in deeper wells indicated flow toward the southern portion of the wetland (toward wells 2 and 4), and outward toward the ocean. The majority of the sites have upward hydraulic gradients, indicating groundwater is discharging to the mangrove swamp. Temperature data recorded at depth of 7 cm, 14 cm and 21 cm indicate a rapid damping of the diurnal temperature signal with depth. These data were best fit to a one-dimensional heat transport model when upward velocities were used to simulate the advective component of temperature transport (Figures 12-15). Upward velocities used to fit the heat transport model to the temperature data ranged from 7.1×10^{-6} to 1.7×10^{-5} m/sec.

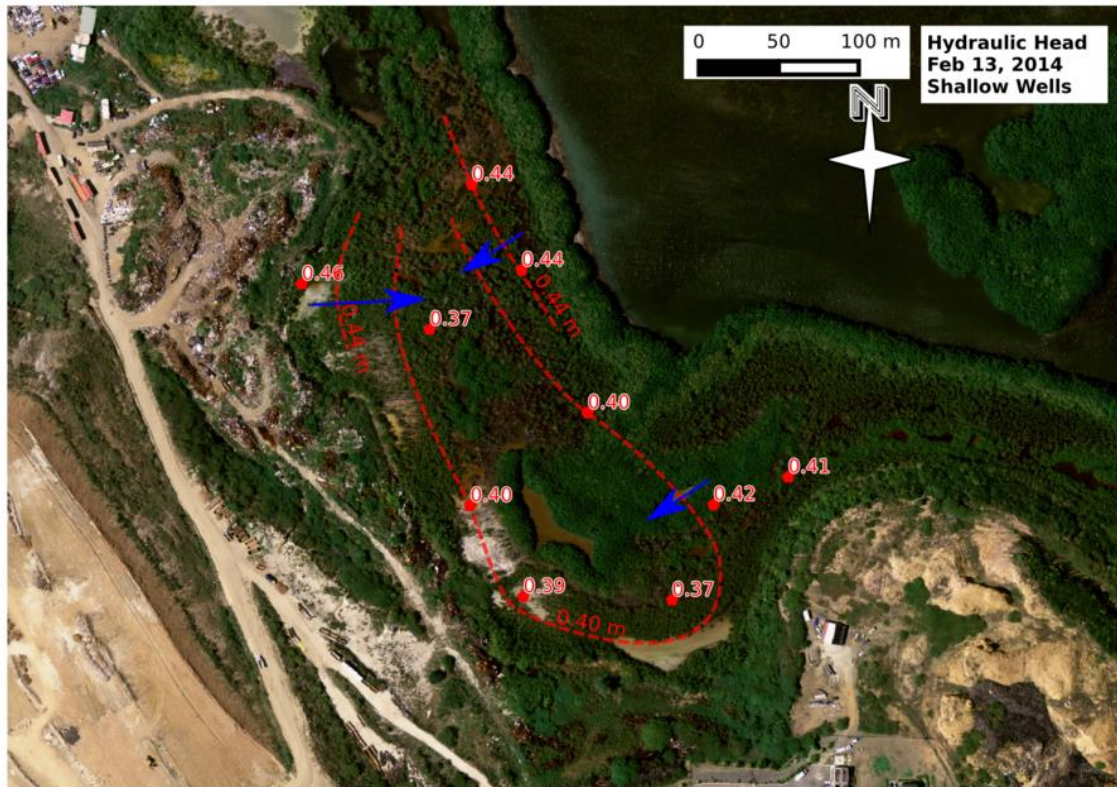


Figure 8. Hydraulic head measurements collected from shallow (1 m deep) wells on February 13, 2014. Equipotentials (dashed red curves) and flow directions (blue arrows) interpreted from the hydraulic head data are superimposed on the well data. Orthophotographs from U.S. Geological Survey (<http://cumulus.cr.usgs.gov>) published Dec. 2010.

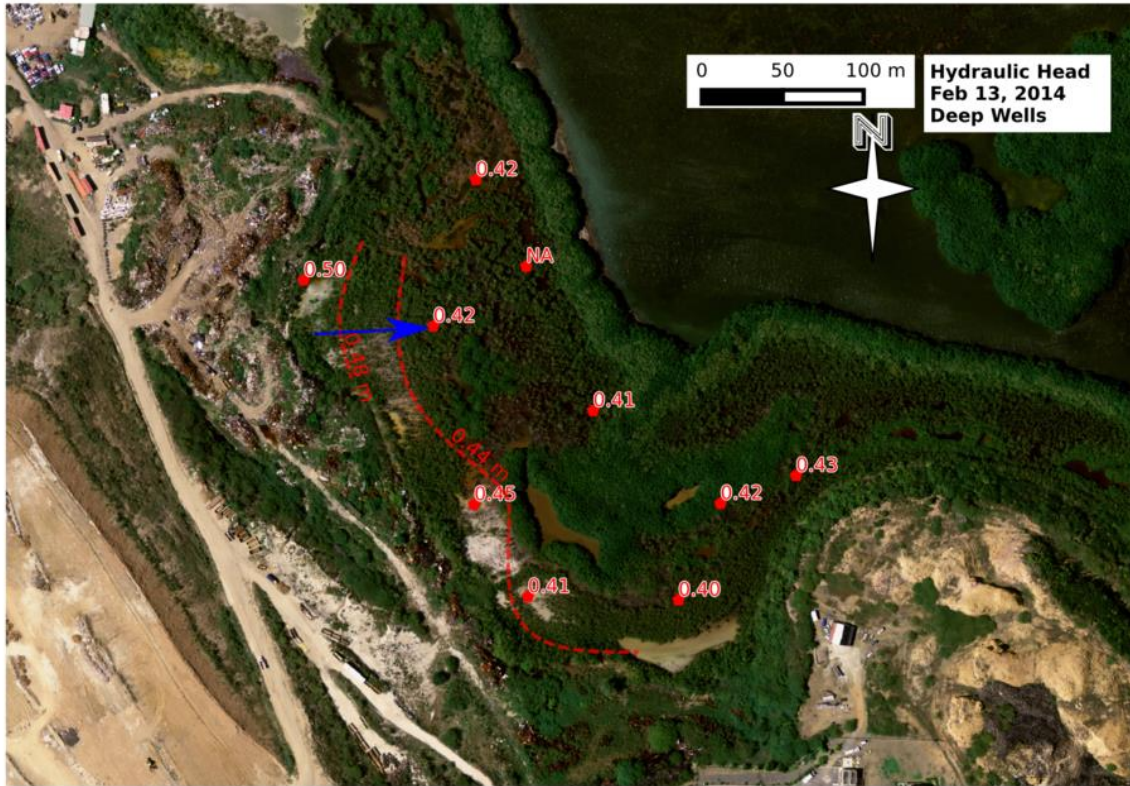


Figure 9. Hydraulic head measurements collected from deep (2.5 m deep) wells on February 13, 2014. Equipotentials (dashed red curves) and flow directions (blue arrows) interpreted from the hydraulic head data are superimposed on the well data. Orthophotographs from U.S. Geological Survey (<http://cumulus.cr.usgs.gov>) published Dec. 2010.

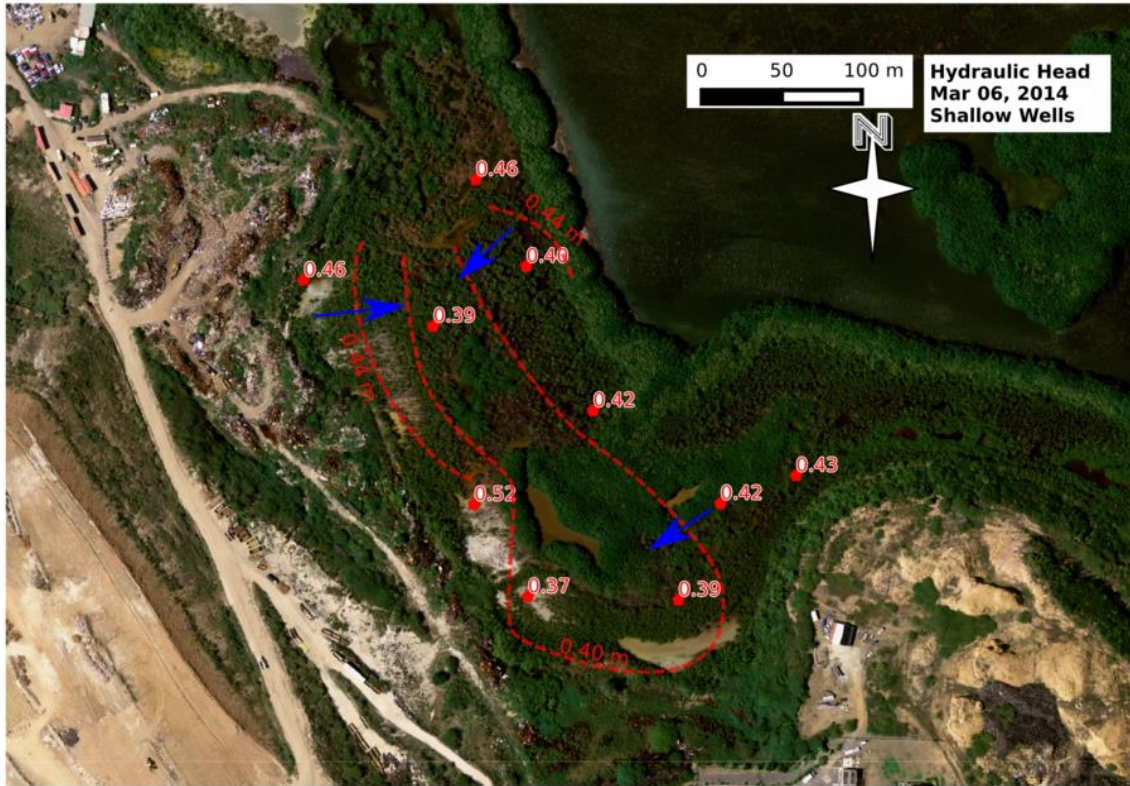


Figure 10. Hydraulic head measurements collected from shallow (1 m deep) wells on March 6, 2014. Equipotentials (dashed red curves) and flow directions (blue arrows) interpreted from the hydraulic head data are superimposed on the well data. Orthophotographs from U.S. Geological Survey (<http://cumulus.cr.usgs.gov>) published Dec. 2010.

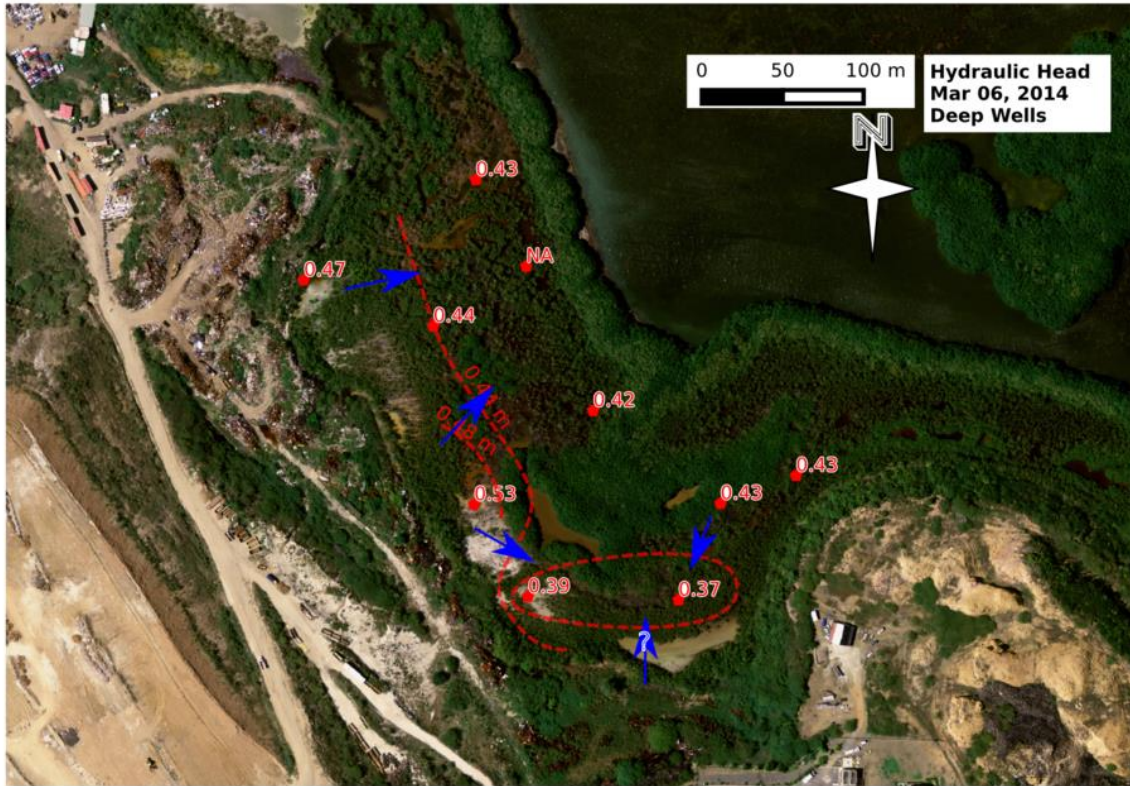


Figure 11. Hydraulic head measurements collected from deep (2.5 m deep) wells on March 6, 2014. Equipotentials (dashed red curves) and flow directions (blue arrows) interpreted from the hydraulic head data are superimposed on the well data. Orthophotographs from U.S. Geological Survey (<http://cumulus.cr.usgs.gov>) published Dec. 2010.

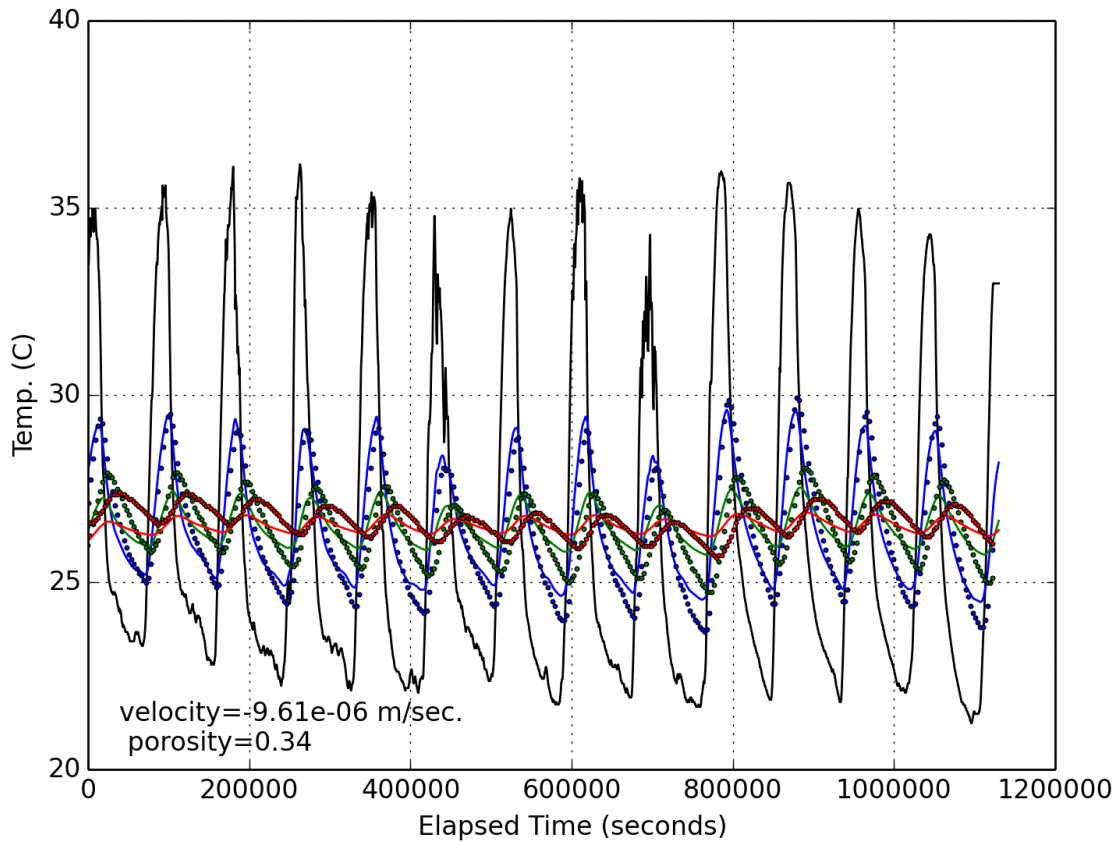


Figure 12. Groundwater temperature data collected at site 5 from February 13 to February 26, 2014. Data were collected at the interface between surface water and sediment (black line), and at depths of 7 cm (blue dots), 14 cm (green dots) and 21 cm (red dots). Blue, green, and red lines display results from a one-dimensional heat transport model at depths of 7, 14, and 21 cm calibrated to the data by varying the groundwater velocity and sediment porosity. The computer simulation best matched the field data when porosity was set to 34% and groundwater velocity was -9.6×10^{-6} m/sec (discharge or upward flow).

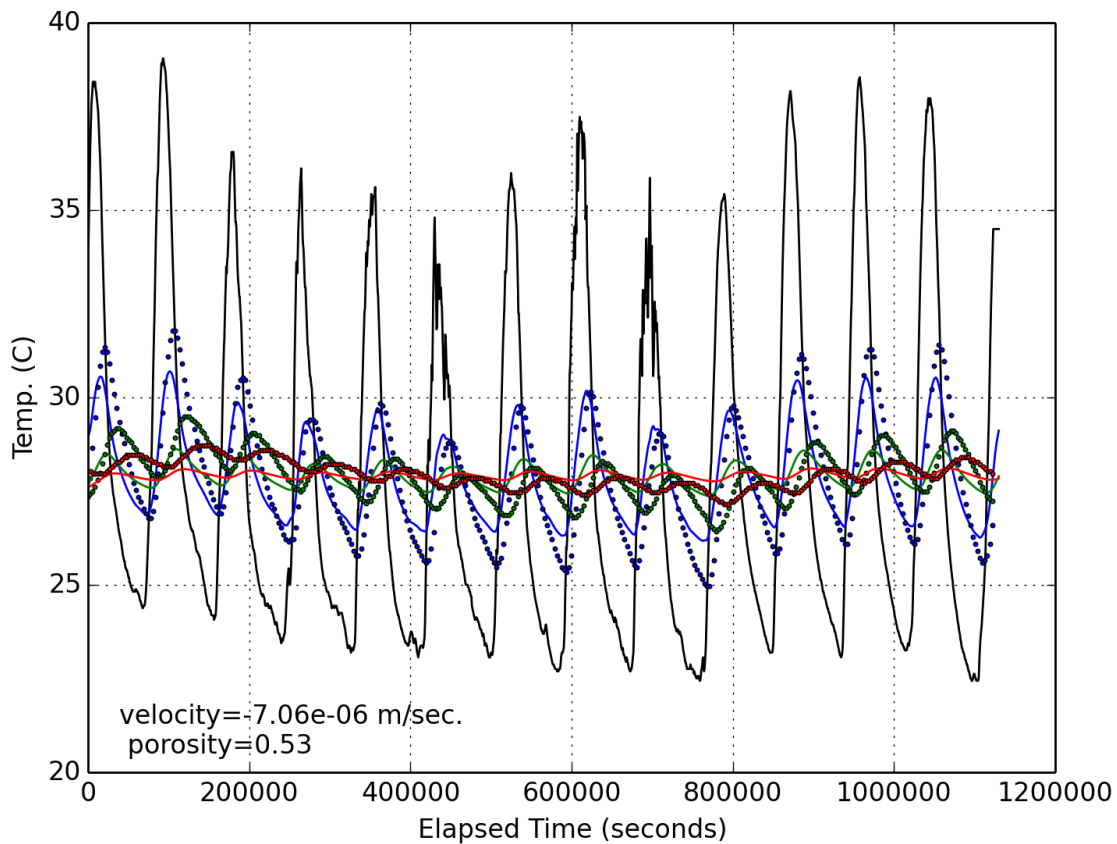


Figure 13. Groundwater temperature data collected at site 7 from February 13 to February 26, 2014. Data were collected at the interface between surface water and sediment (black line), and at depths of 7 cm (blue dots), 14 cm (green dots) and 21 cm (red dots). Blue, green, and red lines display results from a one-dimensional heat transport model at depths of 7, 14, and 21 cm calibrated to the data by varying the groundwater velocity and sediment porosity. The computer simulation best matched the field data when porosity was set to 53% and groundwater velocity was -7.1×10^{-6} m/sec (discharge or upward flow).

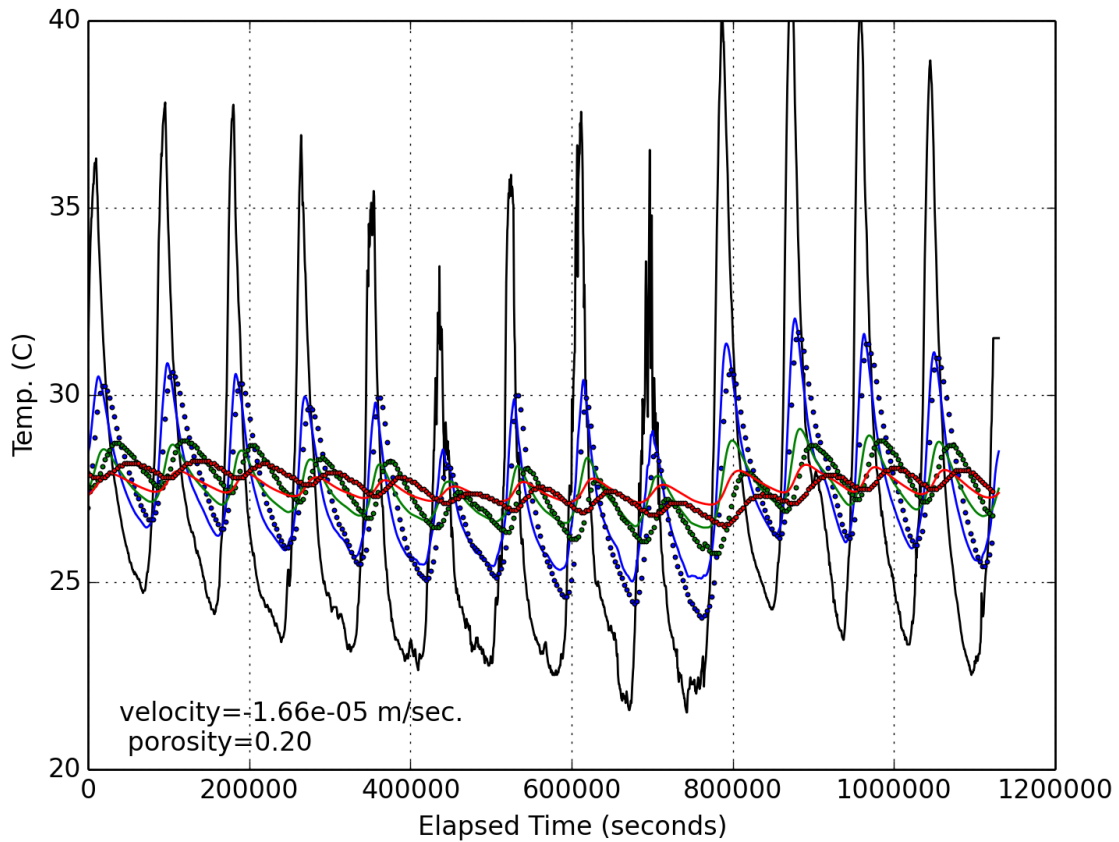


Figure 14. Groundwater temperature data collected at site 1 from February 13 to February 26, 2014. Data were collected at the interface between surface water and sediment (black line), and at depths of 7 cm (blue dots), 14 cm (green dots) and 21 cm (red dots). Blue, green, and red lines display results from a one-dimensional heat transport model at depths of 7, 14, and 21 cm calibrated to the data by varying the groundwater velocity and sediment porosity. The computer simulation best matched the field data when porosity was set to 20% and groundwater velocity was -1.7×10^{-5} m/sec (discharge or upward flow).

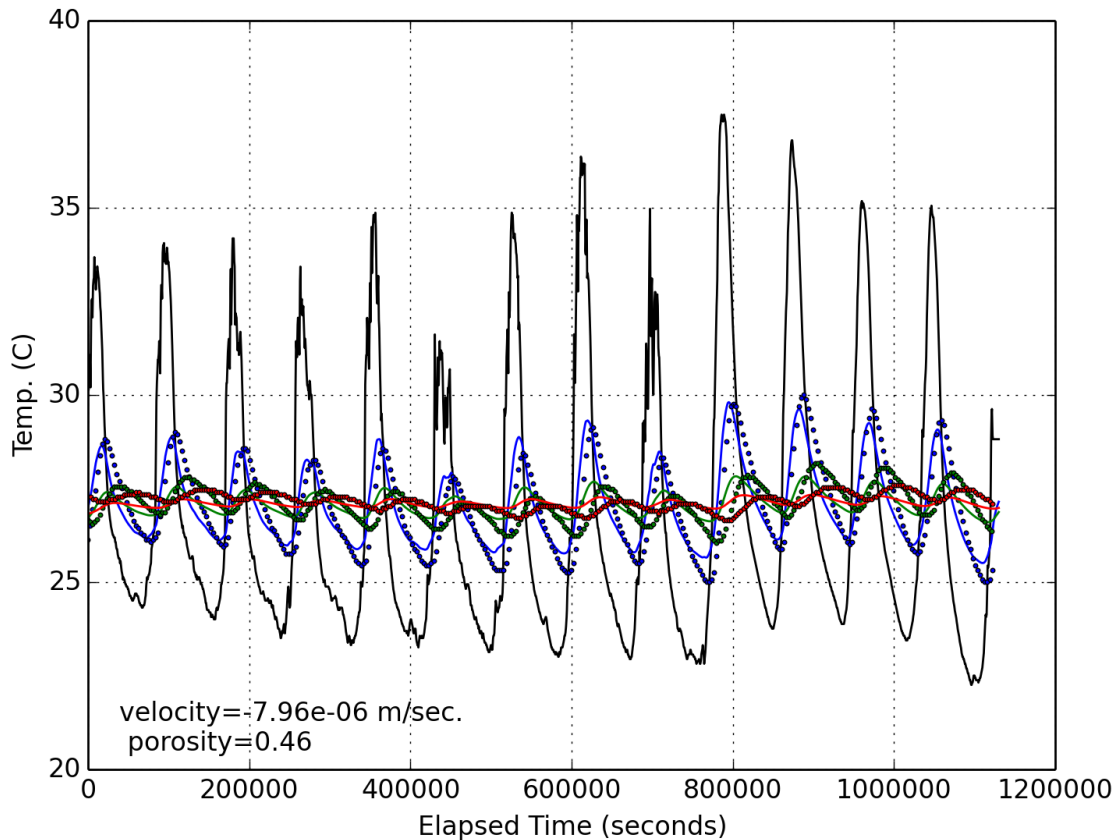


Figure 15. Groundwater temperature data collected at site 2 from Feb. 13 to Feb 26, 2014. Data were collected at the interface between surface water and sediment (black line), and at depths of 7 cm (blue dots), 14 cm (green dots) and 21 cm (red dots). Blue, green, and red lines display results from a one-dimensional heat transport model at depths of 7, 14, and 21 cm calibrated to the data by varying the groundwater velocity and sediment porosity. The computer simulation best matched the field data when porosity was set to 46% and groundwater velocity was -8.0×10^{-6} m/sec (discharge or upward flow).

Time series water level data recorded at 20 minute intervals (Figures 16-25) display a monthly signal, with a rapid increase in water levels followed by a month-long decline in water level. Data archived for the Bovoni Weather Station by Weather Underground (www.wunderground.com) indicate rainfall amounts exceeding 0.2 inches on January 12, 2014 (0.22 in) and February 22, 2014 (0.68 in). Predicted ocean tidal range peaked on January 13, 2014 (-0.4 to 0.8 ft), January 29, 2014 (-0.4 to 1.0 ft), February 11, 2014 (-0.4 to 0.7 ft), and February 26, 2014 (-0.3 to 0.9 ft). Rapid increases in water levels were recorded in data logging pressure sensors on January 28, February 22, February 26, 2014 indicating that rapid influx of water into the mangrove swamp occurs during the highest tides and during high rainfall events. These rapid changes in water level suggest the mangrove swamp is hydraulically isolated from

the ocean.

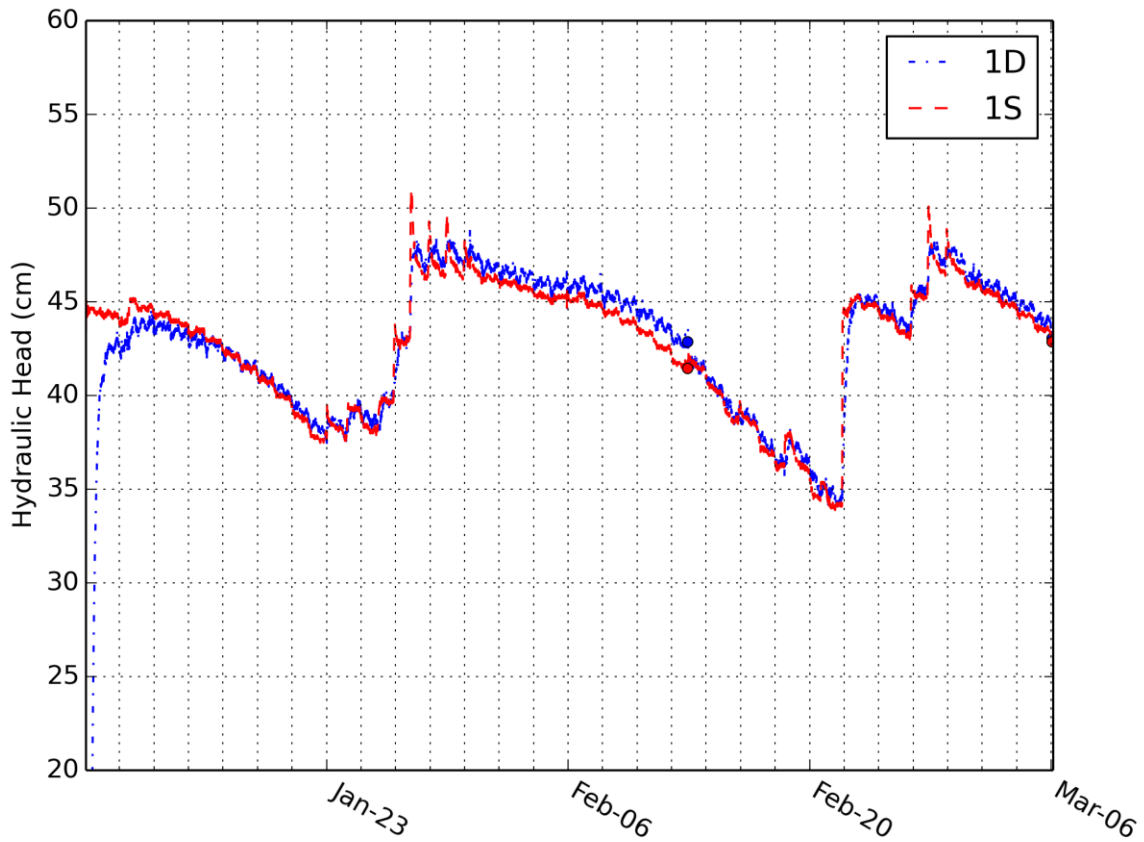


Figure 16. Time series of hydraulic head data at site 1 from January 9 to March 06, 2014 measured manually (dots) and recorded with a data logging pressure transducer (lines). Hydraulic head in shallow (red) wells are typically lower than in deep (blue) wells, indicating groundwater discharge at this location to the mangrove swamp.

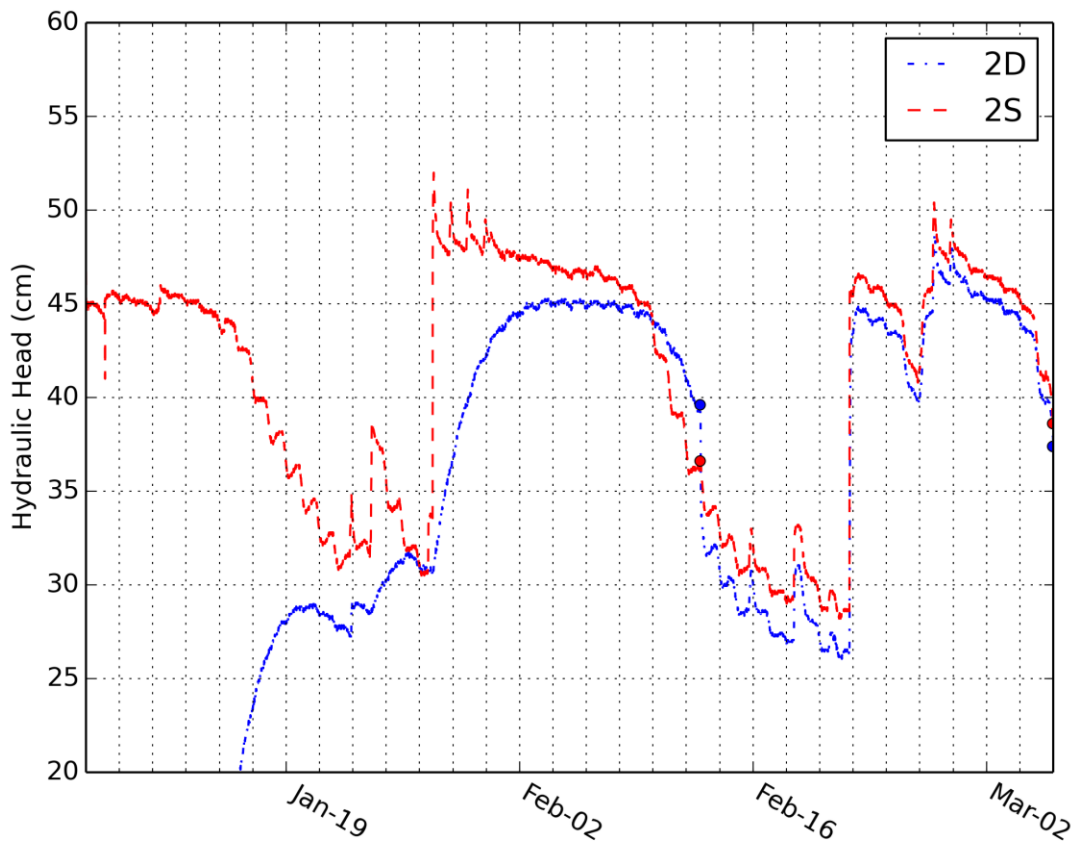


Figure 17. Time series of hydraulic head data at site 2 from January 9 to March 6, 2014 measured manually (dots) and recorded with a data logging pressure transducer (lines). Hydraulic head in shallow (red) and deep (blue) wells indicating vertical groundwater flow at this location oscillates from recharge to discharge over time. Low hydraulic head values in the deep well (before February 2, 2014) are due to the slow influx of water into the well after installation as the well equilibrated.

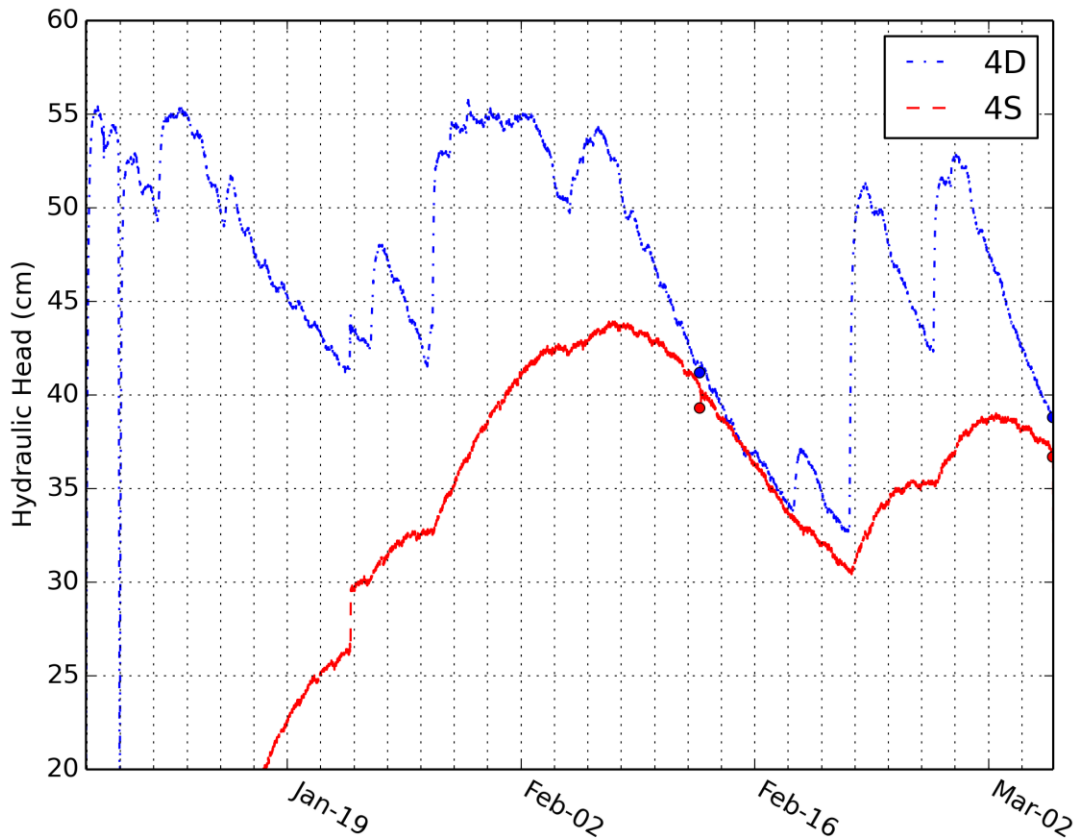


Figure 18. Time series of hydraulic head data at site 4 from January 7 to March 6, 2014 measured manually (dots) and recorded with a data logging pressure transducer (lines). Hydraulic head in shallow (red) well is lower than that in the deep (blue) well indicating groundwater discharge at this location to the mangrove swamp. Low hydraulic head values in the shallow well (before January 29, 2014) are due to the slow influx of water into the well after installation as the well equilibrated.

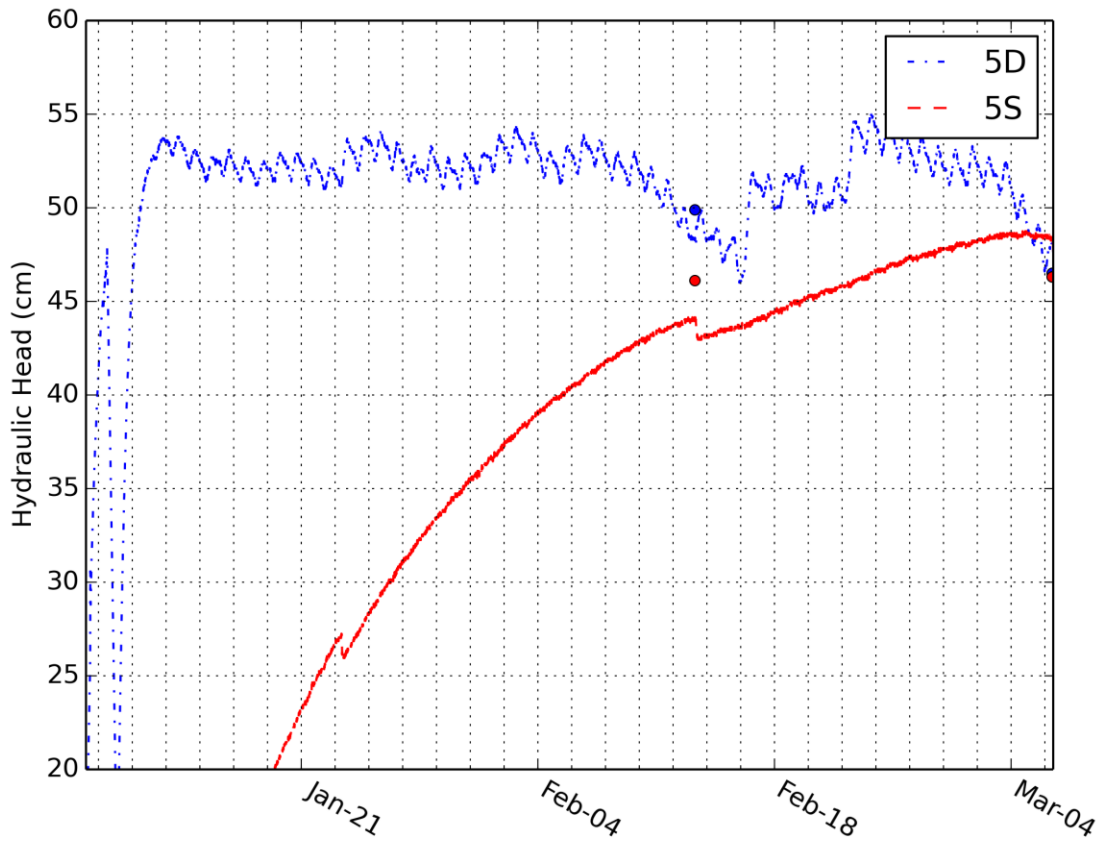


Figure 19. Time series of hydraulic head data at site 5 from January 9 to March 6, 2014 measured manually (dots) and recorded with a data logging pressure transducer (lines). Low hydraulic head values in the shallow (red) well (entire plot) are due to the slow influx of water into the well after installation as the well equilibrated.

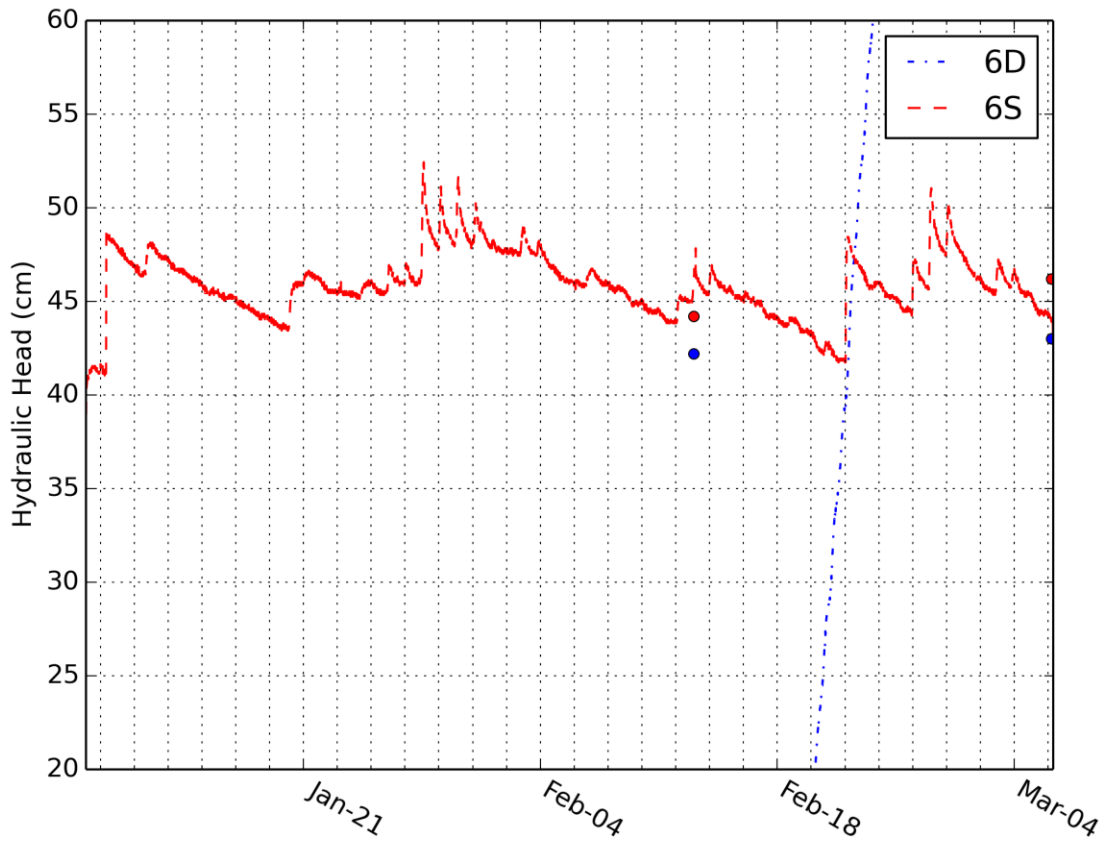


Figure 20. Time series of hydraulic head data at site 6 from January 9 to March 6, 2014 measured manually (dots) and recorded with a data logging pressure transducer (lines). Manual hydraulic head measurements indicate hydraulic heads in the deep (blue) well are lower than in the shallow well, indicating groundwater discharge at this location to the mangrove swamp. The data logging pressure transducer installed in the deep well appears to be malfunctioning and is not recording reasonable hydraulic head data.

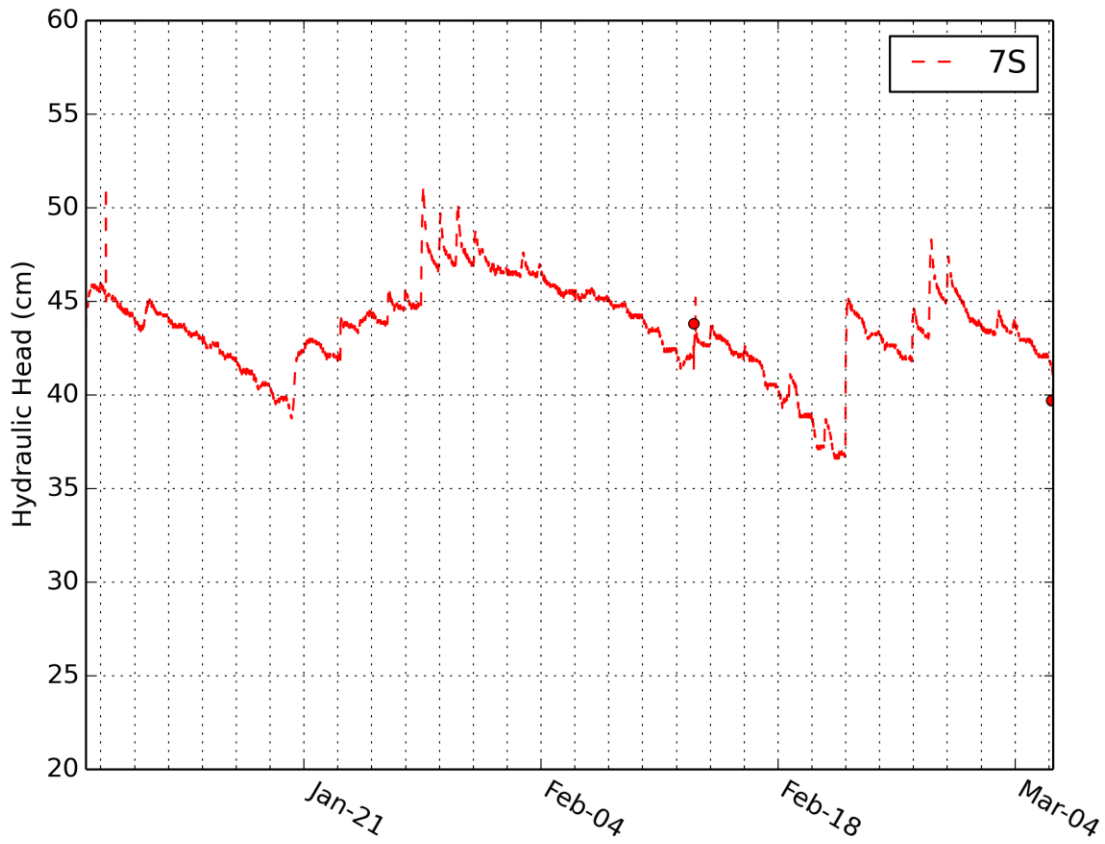


Figure 21. Time series of hydraulic head data at site 7 from January 9 to March 6, 2014 measured manually (dots) and recorded with a data logging pressure transducer (line).

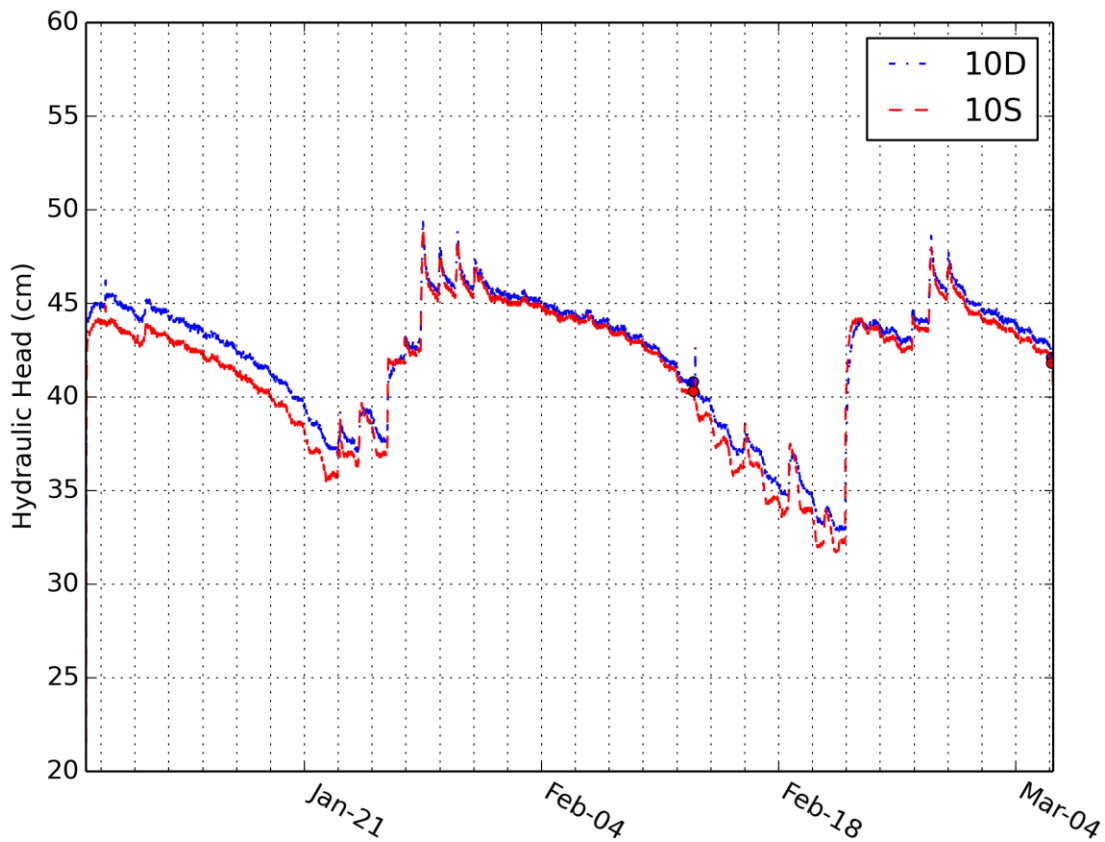


Figure 22. Time series of hydraulic head data at site 10 from January 7 to March 6, 2014 measured manually (dots) and recorded with a data logging pressure transducer (lines). Hydraulic head in shallow (red) well is lower than that in the deep (blue) well indicating groundwater discharge at this location to the mangrove swamp.

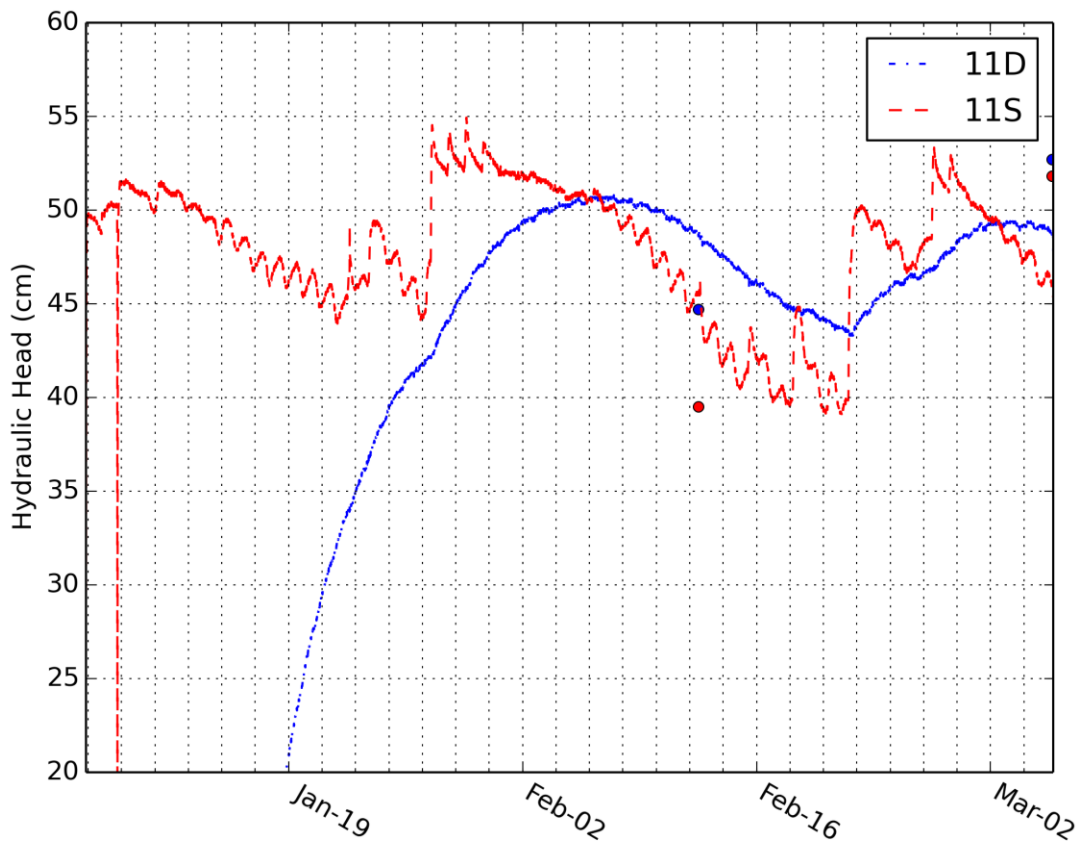


Figure 23. Time series of hydraulic head data at site 11 from January 7 to March 6, 2014 measured manually (dots) and recorded with a data logging pressure transducer (lines). Hydraulic head in shallow (red) well is varies above and below than that in the deep (blue) well indicating shifts in the direction of vertical groundwater flux at this location. Low hydraulic head values in the deep well (before January 29, 2014) are due to the slow influx of water into the well after installation as the well equilibrated.

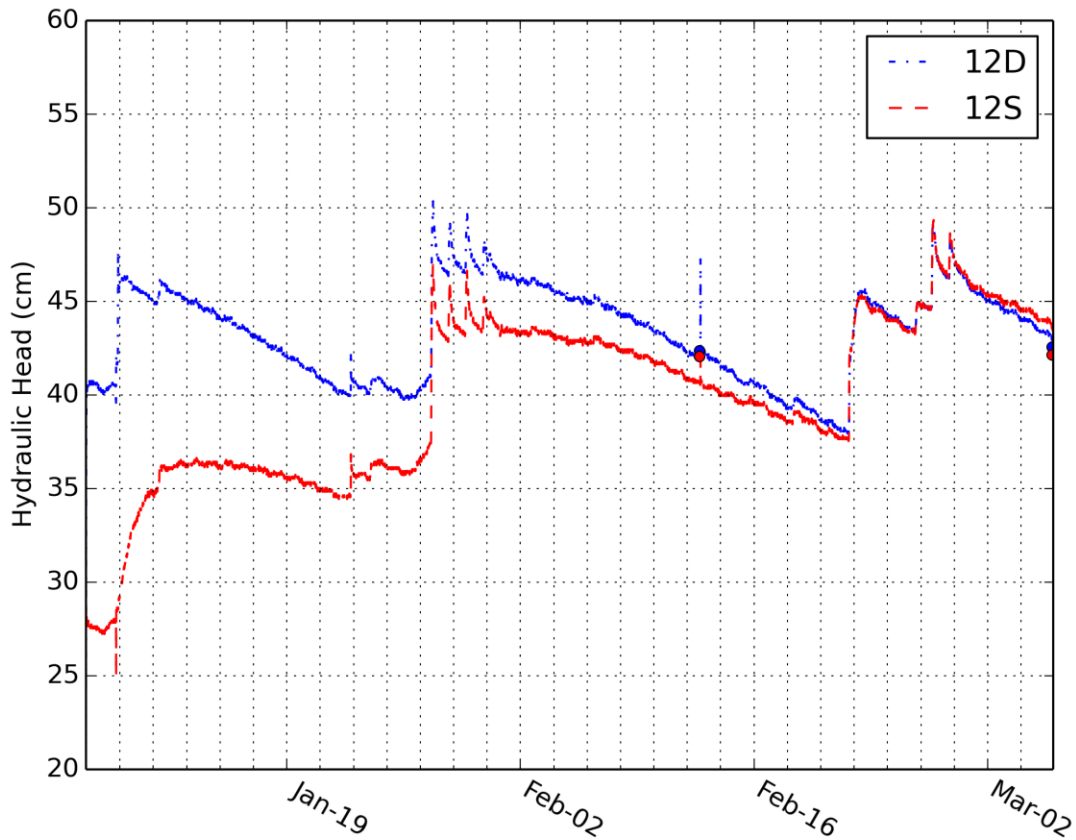


Figure 24. Time series of hydraulic head data at site 12 from January 7 to March 6, 2014 measured manually (dots) and recorded with a data logging pressure transducer (lines). Hydraulic head in shallow (red) well is usually lower than that in the deep (blue) well indicating groundwater discharge to the mangrove swamp. Low hydraulic head values in the shallow well (before January 29, 2014) are due to the slow influx of water into the well after installation as the well equilibrated.

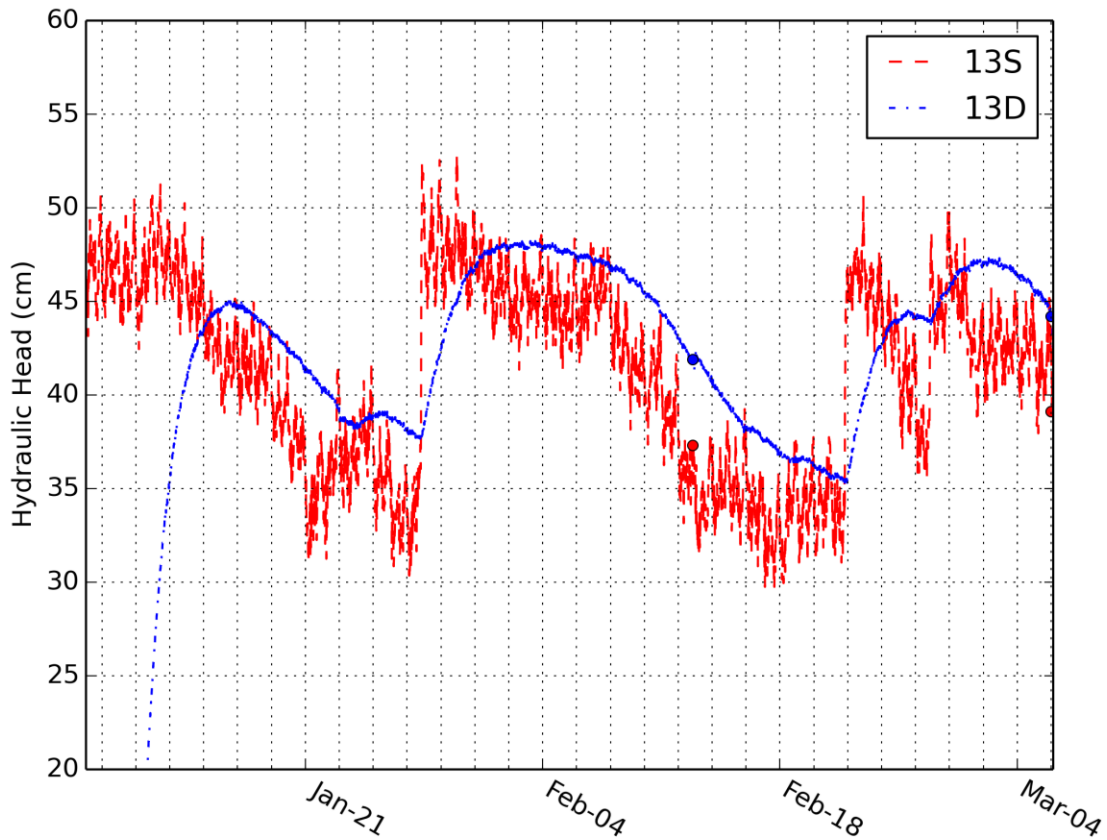


Figure 25. Time series of hydraulic head data at site 13 from January 7 to March 6, 2014 measured manually (dots) and recorded with a data logging pressure transducer (lines). Hydraulic head in shallow (red) well is usually lower than that in the deep (blue) well indicating groundwater discharge to the mangrove swamp. Oscillations in shallow well data occur twice a day and appear to be related to ocean tides.

Slow recovery of water levels in many of the wells (2 deep, 4 shallow, 5 shallow, 11 deep, and 13 deep) may be due to their installation in very low permeability sediment which preliminary observations of geologic cores support. Alternatively, the well screens may have become clogged with sediment despite efforts to scrub them and surge water into the well to clear sediment from the screen. Applying the Hvorslev method and assuming a 37% recovery of water over one day in a 2.5 cm diameter well with a 30 cm long screen results in a hydraulic conductivity of about 10^{-8} m/sec. This low hydraulic conductivity material (consistent with values for silt or clay), where present, will limit the rate of groundwater exchange with the mangrove swamp system.

4.3 Water Chemistry

Surface water salinities varied across the study area from mesohaline at site 5 to metahaline at sites 2 and 7 (Table 1). Specific conductance varied from 7.3 (mS/cm) in the surface ditch to 101.2 (mS/cm) in the site 5 deep well (Table 2). Samples varied in pH from 6.60-9.09 (Table 2). The surface ditch and site 5 shallow well were more basic than other sampled sites.

Table 1. Surface water salinities collected in the field on January 9, 2014 varied across the study area. The handheld meter did not record salinity at sites 4, 6, and 13.

Well Site	Date Sampled	Surface Water Salinity (psu)
1	1/9/2014	No data
2	1/9/2014	42.7
4	1/9/2014	---
5	1/9/2014	5.1
6	1/9/2014	---
7	1/9/2014	47.2
10	1/9/2014	32.5
11	1/9/2014	32.3
12	1/9/2014	35.1
13	1/9/2014	---

Table 2. Specific conductance and pH for water samples. All data were measured on the day of collection using handheld electrical probes (1/9/2014). Calibration of the pH meter was done using pH 4 and 7 standards. Calibration of the specific conductance meter was done using standards with conductivities of 1., 1.9, and 18 mS/cm.

Sample ID	pH	Sp.Cond
	Std.Units.	(mS/cm)
1 Deep	6.65	71.7
1 Shallow	6.70	70.3
11 Deep	7.41	74.0
11 Shallow	6.92	84.6
2 Deep	6.93	86.9
2 Shallow	6.70	90.0
4 Deep	6.60	72.3
4 Shallow	7.46	58.6
5 Deep	6.75	101.2
5 Deep duplicate	6.82	not measured
5 Surface	9.09	12.9
5 Surface duplicate	9.13	not measured
Surface Ditch	8.02	7.3

Total dissolved nitrogen (TDN) concentrations ranged from 120 mg/l in the surface ditch at the edge of the Bovoni Landfill to 4.45 mg/l in the deep well at site 1 (Figure 26, Table 3). The site 2 shallow well, site 5 surface water and deep well, and site 11 shallow had TDN concentrations ranging from 14.1-20.9 mg/l, which were much lower than the surface ditch, but greater than other sampled wells (Table 3).

Most samples contained heavy metal concentrations below analytical detection limits (Table 3). Nickel was measured at site 5 deep (82.2 ppb), 5 shallow (82.2 ppb), 5 surface water (130 ppb), and in the surface ditch adjacent to the landfill (99 ppb). Zinc was detected in the water sample collected at site 5 surface (67.7 ppb). Tin (99 ppb) was detected in the surface ditch water sample. Chromium concentrations were above reporting limits at all sites and ranged from 23.4 to 74.5 ppb, with the highest concentrations measured in samples collected at site 5 deep and the surface.

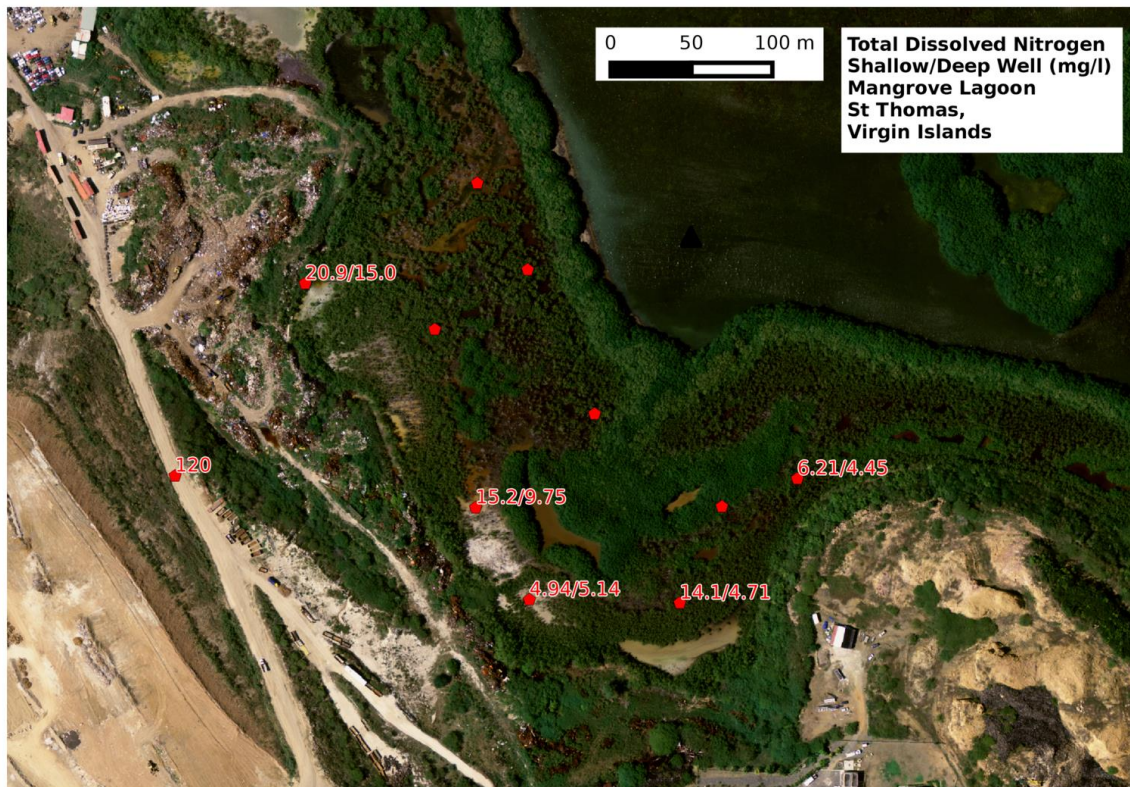


Figure 26. Total dissolved nitrogen concentrations measured at monitoring well locations and a surface ditch near the Bovoni Landfill. The ‘Ditch’ sample and the shallow sample at site 5 were collected from surface water and all other samples were collected from groundwater wells. Orthophotographs from U.S. Geological Survey (<http://cumulus.cr.usgs.gov>) published Dec. 2010.

Table 3. Chemistry data for filtered (0.45 um) water samples. Chemical analyses were performed at the University of Maine’s Sawyer Environmental Chemistry Laboratory. Metals analyses were completed by Inductively Coupled Plasma Atomic Emission Spectroscopy and Total Dissolved Nitrogen (TDN) analysis was performed with an ALPKEM flow solution IV autoanalyzer. RL stands for Recording Limit.

			Dissolved Metals					
		TDN	Cu	Cr	Ni	Pb	Sn	Zn
Sample ID	Date	mg/L	µg/L	µg/L	µg/L	µg/L	µg/L	µg/L
<i>Reporting Limit</i>	-	0.1	100	20	40	80	100	40
Site 1 Shallow	1/9/2014	6.21	<RL	35.5	<RL	<RL	<RL	<RL
Site 1 Deep	1/9/2014	4.45	<RL	39.2	<RL	<RL	<RL	<RL
Site 2 Shallow	1/9/2014	14.1	<RL	47.1	<RL	<RL	<RL	<RL
Site 2 Deep	1/9/2014	4.71	<RL	41.7	<RL	<RL	<RL	<RL
Site 4 Shallow	1/9/2014	4.94	<RL	23.4	<RL	<RL	<RL	<RL
Site 4 Deep	1/9/2014	5.14	<RL	30.9	<RL	<RL	<RL	<RL
Site 5 Surface	1/9/2014	20.9	<RL	37.3	130	<RL	<RL	67.7
Site 5 Shallow	1/9/2014	--	<RL	33.5	82.2	<RL	<RL	<RL
Site 5 Deep	1/9/2014	15.0	<RL	51.7	<RL	<RL	<RL	<RL
Site 11 Shallow	1/9/2014	15.2	<RL	47.1	<RL	<RL	<RL	<RL
Site 11 Deep	1/9/2014	9.75	<RL	35.4	<RL	<RL	<RL	<RL
Surface Ditch	1/9/2014	120	<RL	74.5	99	<RL	105	<RL
Filter Blank	--	<0.05	<RL	<RL	<RL	<RL	<RL	<RL

5. CONCLUSIONS AND RECOMMENDATIONS

Water levels within the mangrove fringe were lower at its center, indicating that surface waters and shallow groundwater move toward the center of the study area. These low water levels suggest the mangrove swamp is isolated from the ocean by the thin strip of land visible in the aerial images, and that evaporation within the swamp is lowering water levels. This process may also be partly responsible for the discharge of groundwater to the lagoon. We hypothesize that this may be one mechanism resulting in the standing dead mangrove and open-water and muddy areas observed to occur within the mangrove fringe (Figure 5). Additional monitoring and measurements are needed to better understand this potential mechanism.

Groundwater discharge is likely also driven by groundwater mounding beneath Bovoni Landfill and other uplands adjacent to the mangrove swamp. The difference in hydraulic head between an upland and wetland (or surface water) system commonly drives groundwater discharge near the break in hydraulic gradient near the interface between the upland and surface water system. Despite strong evidence for groundwater discharge, supported by both hydraulic head and temperature data, the low hydraulic conductivity of silty sediments in portions of the mangrove swamp may limit the volume of groundwater that flows into the study area. Future work should concentrate on better understanding the geophysical context of the study region through analyses of the geologic cores that were collected and archived in January 2014, including description of lithologic units, bulk density, and organic content, using loss on ignition (LOI) techniques. These data could then be used to describe the subsurface hydrogeologic environment and to assess potential stratigraphic control of groundwater flow paths. UVI graduate student, Jessica Keller, plans to complete these analyses during Summer 2014, as part of her Masters' thesis (beyond the time frame of this pilot study).

Groundwater chemistry data suggest that site 5 receives runoff with elevated concentrations of heavy metals and nutrients. High concentrations of heavy metals and total dissolved nitrogen were not measured in the deeper groundwater wells, suggesting groundwater is not an important pathway for heavy metal and nutrient to the mangrove swamp from nearby sources. However, water chemistry data from surface samples and shallow wells indicate that surface discharge is likely the most important pathway for contaminants to enter the mangrove swamp. At this time, the source and pathway for contaminants within the surface water ditch adjacent to Bovoni Landfill, remain unclear. Future work should include additional water chemistry sampling with greater spatial and temporal resolution throughout the mangrove wetland and surrounding areas.

Finally, this work would benefit from additional modelling of groundwater flow paths using either FiPy (Guyer et al., 2009), a flexible computer modeling package, or the USGS SEAWAT (Langevin et al., 2007) modeling software to create simple, cross-sectional computer models of the mangrove system. FiPy has been used successfully to evaluate groundwater flow problems

in peatland settings (an appropriate analogue; Reeve et al., 2009) and has the ability to vary governing equations to test alternative assumptions regarding groundwater flow and to simulate a variety of processes (groundwater flow, subsurface composition, surface water flow). The SEAWAT computer software could be used when the flexibility of FiPy is not needed or to compare with FiPy simulation to verify that this non-standard modeling system is performing properly.

BIBLIOGRAPHY

Anderson, Mary, 2005, *Heat as a ground water tracer*, Ground Water, 43, 951-968.

Christensen, Thomas, Peter Kjeldsen, Hans-Jorgen Albrechtsen, Gorm Heron, Per Nielson, Poul Bjerg, and Peter Holm, 1994, *Attenuation of landfill leachate pollutants in aquifers*, Critical Reviews in Environmental Science and Technology, 24(2), 119-202.

Conservation Data Center, 2010, *Wetlands of the U.S. Virgin Islands*, Division of Environmental Protection, Department of Planning & Natural Resources, U.S. Virgin Islands.

Costanza, Robert, Ralph d'Arge, Rudolf de Groot, Stephen Farber, Monica Grasso, Bruce Hannon, Karin Limburg, Shahid Naeem, Robert O'Niell, Jose Paruelo, Robert Raskin, Paul Sutton, and Marjan van den Belt, 1997, *The value of the world's ecosystem services and natural capital*, Nature, 387, 253-260.

Dosis, Ioannis, Athanasios Kamarianos, Maria Athanasiadou, Ioannis Athanassiadis, and Xanthippos Karamanlis, 2011, *Polybrominated diphenyl ethers (PBDEs) in marine sediment of Thermaikos Gulf, Greece*, International Journal of Environmental Analytical Chemistry, 91(12), 1151-1165.

Environmental Protection Agency, 2010, *Municipal solid waste in the United States*, Available: <http://www.epa.gov/osw/nonhaz/municipal/pubs/msw2009rpt.pdf>

Federal Register, 2012, *Notice of lodging of consent decree under the Resource Conservation and Recovery Act and Clean Air Act*, Federal Register ,77(59), 18266.

Gobler, Christopher and George Boneillo, 2003, *Impacts of anthropogenically influenced groundwater seepage on water chemistry and phytoplankton dynamics within a coastal marine system*, Marine Ecology Progress Series, 255, 101-114.

Jaluria, Yogesh, 1997, *Computing methods for engineering*, Taylor and Francis, New York 520 p.

Jones, Ross, 2010, *Environmental contamination associated with a marine landfill ('seafill') beside a coral reef*, Marine Pollution Bulletin, 60(11), 1993-2006.

Jones, Eric, Travis Oliphant and Pearu Peterson, 2001-, *SciPy: Open source scientific tools for Python*, available at <http://www.scipy.org>

Klinck, B.A. and Stuart, M.E, 1999, *Human health risk in relation to landfill leachate quality*, Technical report WC/99/17, British Geological Survey, DFID Project No. R6532.

Orth, Robert, Tim Carruthers, William Dennison, Carlos Duarte, James Fourqurean, Kenneth Heck Jr., Randall Hughes, Gary Kendrick, Judson Kenworthy, Suzanne Olyarnik, Frederick Short, Michelle Waycott, and Susan Williams, 2006, *A global crisis for seagrass systems*, *BioScience*, 56(12), 987-996.

Pope, Nick, S O'Hara, M. Imamura, Tom Hutchinson, and William Langston, 2011, *Influence of a collapsed coastal landfill on metal levels in sediments and biota – a portent for the future?* *Journal of Environmental Monitoring*, 13(7), 1961-1974.

Quinn, Brian, Francois Gagne, Jean-Philippe Weber, Christian Blaise, 2005, *Ecotoxicological effects of a semi-submerged municipal dump (Castle Harbour, Bermuda) on the calico scallop *Agropecten gibbus**. *Marine Pollution Bulletin*, 51(5-7), 534-544.

St. Thomas East End Reserve, 2011, *St. Thomas East End Reserves Management Plan*, St. Thomas, USVI, Available:

www.horsleywitten.com/STEERwatersheds/pdf/managementPlans/STEERManagementPlan/STEER_Management_Plan_Final_low.pdf

Valiela, Ivan, Jennifer Bowen, and Joanna York, 2001, *Mangrove forests: one of the world's threatened major tropical environments*, *Bioscience*, 51(10), 807-815.

van Rossum, Guido and Fred Drake (eds), 2001, *Python Reference Manual*, PythonLabs, Virginia, USA, 2001. Available at <http://www.python.org>

Virgin Islands Ecotours, 2012, *Virgin Islands EcoTours Kayak Snorkel Hike in the beautiful USVI*, Available: <http://www.viecotours.com/>

Virgin Islands Waste Management Authority, 2012, *Landfill Operating Policies*, Available: www.viwma.org/business_information/solid_waste_2/landfill_operating_policies.aspx

Zhu, C., R. H. Byrd and J. Nocedal, 1997, L-BFGS-B: Algorithm 778: L-BFGS-B, FORTRAN routines for large scale bound constrained optimization, *ACM Transactions on Mathematical Software*, 23(4),550 - 560.